AD_____

Award Number: DAMD17-00-1-0071

TITLE: Genetics of Bone Mineralization and Morphology in Inbred Mice: Analysis of the HcB/Dem Recombinant Congenic Strains

PRINCIPAL INVESTIGATOR: Robert D. Blank, M.D., Ph.D.

CONTRACTING ORGANIZATION: University of Wisconsin, Madison
Madison, Wisconsin 53706-1490

REPORT DATE: April 2002

TYPE OF REPORT: Annual

PREPARED FOR: U.S. Army Medical Research and Materiel Command
Fort Detrick, Maryland 21702-5012

REPORT DOCUMENTATION PAGE

Form Approved
OMB No. 074-0188

1. AGENCY USE ONLY (Leave blank)	2. REPORT DATE	3. REPORT TYPE AND DATES COVERED
	April 2002	Annual (1 Apr 01 - 31 Mar 02)

4. TITLE AND SUBTITLE
Genetics of Bone Mineralization and Morphology in Inbred Mice: Analysis of the HcB/Dem Recombinant Congenic Strains

5. FUNDING NUMBERS
DAMD17-00-1-0071

6. AUTHOR(S)
Robert D. Blank, M.D., Ph.D.

7. PERFORMING ORGANIZATION NAME(S) AND ADDRESS(ES)
University of Wisconsin, Madison
Madison, Wisconsin 53706-1490

E-Mail:rdb@medicine.wisc.edu

8. PERFORMING ORGANIZATION REPORT NUMBER

9. SPONSORING / MONITORING AGENCY NAME(S) AND ADDRESS(ES)
U.S. Army Medical Research and Materiel Command
Fort Detrick, Maryland 21702-5012

10. SPONSORING / MONITORING AGENCY REPORT NUMBER

11. SUPPLEMENTARY NOTES

12a. DISTRIBUTION / AVAILABILITY STATEMENT
Approved for public release; distribution unlimited

12b. DISTRIBUTION CODE

13. ABSTRACT *(Maximum 200 Words)*

Susceptibility to osteoporotic fractures varies widely with genetic factors accounting for ~50% of this variation. Fracture risk is determined by peak bone mass and skeletal morphology achieved in young adulthood and the rate and extent of bone loss thereafter. This work will analyze the genetics of the first of these components through the use of recombinant congenic mice. We have demonstrated that the 27 HcB/Dem strains differ significantly in a variety of bone strength related phenotypes at 6 months of age. Further, preliminary mapping of genetic loci contributing to these phenotypes has been carried out. An intercross between HcB/13 and HcB/14 will allow more accurate mapping of a subset of these bone strength genes and investigation into pairwise epistatic interactions among loci. A cross examining *Cola2*^{oim}/+ heterozygotes will allow determination of whether segregating differential loci in this system map to the same chromosomal regions identified in the HcB/Dem studies. Further breeding will be performed to develop true congenic lines and refine the mapping of the candidate genes for their positional cloning. Identifying mouse chromosome regions that control peak bone mineralization and morphology will allow prediction of the corresponding human regions by synteny and facilitate human genetic studies of this problem.

14. SUBJECT TERMS
osteoporosis, quantitative traits, epistasis, fracture risk, Biomechanics, biomineralization, bone

15. NUMBER OF PAGES
46

16. PRICE CODE

17. SECURITY CLASSIFICATION OF REPORT	18. SECURITY CLASSIFICATION OF THIS PAGE	19. SECURITY CLASSIFICATION OF ABSTRACT	20. LIMITATION OF ABSTRACT
Unclassified	Unclassified	Unclassified	Unlimited

Table of Contents

INTRODUCTION

The broad purpose of this work is to understand the genetic basis of fracture risk. In order to accomplish this goal, we are working to detect and identify genes whose segregation alters bone biomechanical performance in young adult mice. Two crosses are being analyzed; the first is an intercross of recombinant congenic strains HcB/13 X HcB/14. These strains each carry 1/8 of their genomes from C57BL/10ScSnA and the remainder from C3H/DiSnA. HcB/13 and HcB/14 are highly divergent in their bone properties, but only ~1/4 of the genome segregates in this cross, allowing analysis of epistatic interactions in a moderately sized cross. The second cross is between outbred B6C3/Fe-*a/a-Cola2*$^{oim/+}$ heterozygotes and B6C3/Fe-*a/a* F1 animals. The B6C3 background is closely related to the HcB/Dem system. In both cases, bones from 4 month animals will be phenotyped by 3-point bend testing, radiographic analysis, ash percentage, Fourier-transformed infrared spectroscopy, and histomorphometry. Histograms of the trait values will be used to select animals for use in linkage mapping, which will then be carried out using the QTL Cartographer software suite. Linkage mapping of distributed microsatellite markers will be supplemented by markers isolated through representational difference analysis of phenotypically extreme animals from each cross. QTLs identified in both crosses will be isolated through the generation of congenic lines by marker-assisted selection. The approach taken in this work expands on earlier investigations of bone genetics in that biomechanical performance is a primary endpoint and that pleiotropy testing of biomechanical outcomes and sub-phenotypes relates QTLs to specific components of bone strength.

BODY

Statement of Work Item 1: Intercross between HcB/13 and HcB/14

Progress on this item was delayed approximately 6 months last year due to issues arising from my relocation to the University of Wisconsin. In last year's progress report, we anticipated being able to make up approximately 3 months during the past year.

We have genotyped approximately 50 additional markers in the HcB/Dem strains. We expect that an additional 50 markers will be analyzed within the next 2 months. This will accomplish the additional genotyping portion of aim 1. The delay in completing the genotyping is due not to a problem, but to simultaneous performance of the Aim 1 genotyping and the Aim 2 genotyping (see next section).

We have generated the 13 X 14 and 14 X 13 F1 populations. We have generated approximately ~2/3 of the 13 X 14 arm of the F2 population, but only ~1/10 of the 14 X 13 arm of the F2 population. In the statement of work, we specified that a reciprocal cross would be generated and analyzed. The poor breeding of the 14 X 13 arm relative to the 13 X 14 arm demonstrates the biological differences arising from whether specific alleles are inherited maternally or paternally. In order to overcome this breeding problem, we have increased the number of 14 X 13 F1 matings. We expect all mice to be bred and sacrificed by mid-autumn. We expect micro-CT and mechanical testing to be completed by the end of 2002.

Statement of Work Item 2: Genetic Characterization of Col1a2$^{oim/+}$ heterozygotes

Two completementary approaches are being pursued to achieve this aim. The first is to genotype our previously generated population of 225 *Col1a2*$^{oim/+}$ heterozygotes using informative microsatellite markers and use these genotypes and phenotypic data from these animals to map modifiers of bone strength. The second is to generate markers linked to putative modifiers of bone strength by representational difference analysis (RDA). We have made progress using both approaches.

We have completed approximately ½ of the microsatellite marker genotyping for the population and expect this to be completed sometime in June. Linkage analysis once the genotypes have been generated will require less than 1 month. We have exploited the observation of phenotypic attenuation of *Col1a2*$^{oim/oim}$ homozygotes by using the outbred and partially inbred *Col1a2*$^{oim/oim}$ animals to generate the DNA pools for this task, rather than the extreme animals of the *Col1a2*$^{oim/+}$ heterozygote population. We have generated collections of fully subtracted clones using 2 different restriction enzymes. Subtraction is still in progress with a 3rd restriction enzyme. We are presently characterizing the clones obtained to date, in order to limit testing these for association with bone strength to those shown not to be repetitive sequences, cloning artifacts, or sequences that escaped subtraction. We expect to have completed the RDA experiments, including tests of association by mid-autumn of 2002. It should be noted that use of the outbred and partially inbred *Col1a2*$^{oim/oim}$ animals to perform this experiment strengthens the experiment, as different populations of animals are being used to generate (homozygotes) and test (heterozygotes) RDA-derived markers for association with bone strength.

Statement of Work Item 3: Initiation of Breeding to Generate Congenic Lines

This aspect has not yet begun, as it is contingent on mapping data from statement of work item 1. This was not expected to begin until late in year 3 or year 4, and we do not believe that this timetable requires modification.

Modification of Statement of Work in View of Research Performed to Date

Three changes in the statement of work are proposed as a result of the past year's events:

First, the timeline for the intercross must be extended because of the poor breeding performance in the HcB/14 X HcB/13 arm of the cross. This delays task c of item 1 by 6 to 9 months. Item d of item 1 will be delayed approximately 3 months. Items e and f are not expected to be delayed.

Second, item 2's RDA experiments have been performed with outbred and partially inbred *Col1a2*$^{oim/oim}$ animals rather than heterozygous animals as originally proposed. Part c of the item 2 statement of work is approximately 3 months behind schedule. Completion of part d of this item is not expected to be delayed. As noted above, the change in choice of DNAs to be used for this portion of the proposed experiment strengthens the experimental design, as the RDA markers are derived from 1 set of animals and tested in a distinct population.

Third, genotyping and mapping the *Col1a2*$^{oim/+}$ heterozygous animals is progressing nicely and is being done in addition to the items outlined in the original statement of work. We expect that this will be completed sometime in year 3.

KEY RESEARCH ACCOMPLISHMENTS

- Observation that HcB/13 X HcB/14 matings are more productive than HcB/14 X HcB/13 matings.
- Generation of RDA products from outbred and partially inbred *Col1a2*$^{oim/oim}$ pooled DNAs
- Genotyping at ~50 loci for HcB/Dem series and the 225 *Col1a2*$^{oim/+}$ heterozygous animals
- Observation of differences in collagen cross-link maturity and crystallinity between HcB/8 and HcB/23, a pair of strains in which calculated tissue strength differs markedly in spite of similar ash percentages. These FTIR indices, since they are independent of the 5 traits mapped simultaneously in the HcB/Dem strain survey (mass, failure load, structural stiffness, ash percentage, and cross-sectional moment of inertia) can be added to linkage maps in seeking potential pleiotropic bone-strength related loci.

REPORTABLE OUTCOMES

Manuscripts

The preliminary data included in the original application for this award are reported in a manuscript published in *The Journal of Bone and Mineral Research* [1]. This manuscript was in press at the time of last year's report and was included as an appendix at that time.

A perspective [2] arising from a report by Beamer and associates [3] was published in *The Journal of Bone and Mineral Research*. This manuscript was in press at the time of last year's report and was included as an appendix at that time.

The manuscript describing the use of GC-clamps as an aid to the design of denaturing high performance liquid chromatography submitted to *Clinical Chemistry* has still not been published. The reviewers requested significant revisions of the manuscripts– primarily directed at shortening the report to approximately ¼ of its present length. The co-authors have not yet approved the revised manuscript. While not a component of the approved Statement of Work, this work nevertheless could not have been accomplished without this award.

An original manuscript [4] describing the inhibitory effects of sulfate on *in vitro* mineralization was published during the past year. It is included as appendix 1. While not a component of the approved Statement of Work, the investigation was greatly facilitated by this award.

An original manuscript describing Fourier Transform Infrared spectroscopic data from the HcB/8 and HcB/23 recombinant congenic strains is nearly ready for submission. While study of this pair of strains was not included in the approved Statement of Work, the large differences in the calculated tissue strength of bones from these strains prompted our choice of these strains for initial investigation of collagen cross-link maturity and crystallinity in these strains. Support provided by this award was invaluable in performing these studies. A draft is included as appendix 2. Please note that the manuscript still is under review by co-authors and that the discussion will likely be amplified prior to submission.

Abstracts

Representational difference analysis comparison of fully outbred *Cola2*$^{oim/oim}$ homozygotes and partially inbred *Cola2*$^{oim/oim}$ homozygotes was presented as a poster at The American Society for Bone and Mineral Research 2001 annual meeting and was included as an appendix in last year's annual report.

Geometry as a Heritable Determinant of Bone Strength was presented as a poster at The American Society for Bone and Mineral Research 2001 annual meeting and was included as an appendix in last year's annual report.

Genotypic and Phenotypic Characterization of Mouse Bone was presented orally at the Care and Characterization of Genetically Engineered Mice and Comparative Pathology in Functional Genomics Co-Conferences sponsored by the NIH-OLAW and the C.L. Davis, DVM Foundation at The Baylor College of Medicine, February 12-16, 2002. The slides from this presentation were published in the conference proceedings. The file containing the presentation will be provided at your request.

Collagen Cross-Link Maturity and Crystallinity Indices Differ Markedly in Recombinant Congenic Mice Having Divergent Calculated Tissue Strength has been submitted as an abstract to The American Bone and Mineral Research 2002 annual meeting and is included as appendix 3.

Patents and Licenses

None

Degrees Granted

None

Cell Lines and other Biological Reagents

None

Informatics Resources and Models

None

Other Funding

An application entitled "Phenotypic Attenuation in Murine Osteogenesis Imperfecta" was submitted to the NIH and assigned number AR48324. This application, with some modification, was also submitted to the March of Dimes Birth Defects Foundation. Both applications are pending, with funding decisions expected in October, 2002 and May, 2002, respectively. The NIH application was revised to address comments arising from the original submission, which was not funded.

An application entitled "The Role of Genetic Background in Skeletal Adaptation to Increased and Decreased Loading" was submitted by Dr. M. C. H. van der Meulen to NASA and includes me as a consultant. This application relies on the divergence of HcB/13 and HcB/14 bone properties. This application was not funded.

A new application, entitled "Genetics of Bone Tissue Material Properties in Mice" was submitted to the Department of Veterans' Affairs Merit Review program in December, 2001. While a final funding decision is still pending for this application, it was judged on review to be "highly meritorious and likely to receive funding" beginning in October, 2002. A final funding decision is anticipated by July, 2002. The application was modeled on the USAMRAA project and if funded, will allow a second intercross, between HcB/8 and HcB/23 to be undertaken.

In July, 2001, I received a University of Wisconsin/Howard Hughes Medical Institute Faculty Development Award. This 2 year award provides flexible funds.

Employment and other Research Opportunities
None

CONCLUSIONS

While work remains on-track with regard to statement of work item 2, item 1 remains significantly behind schedule. Some of this tardiness arose from my laboratory's relocation to the University of Wisconsin, but in addition to that, one arm of the reciprocal intercross proposed has bred poorly. We expect to complete the proposed overall work on schedule in spite of this.

In addition, the findings that collagen cross-link maturity and crystallinity apparently reflect differences in bone tissue strength have provided a potential mechanism for explaining differences in bone tissue strength that are *independent* of mineral content. This observation is the basis of a highly scored VA Merit Review application in which we will study a reciprocal intercross of HcB/8 and HcB/23, focusing on tissue strength rather than structural strength.

Ultimately, biomechanical performance under physiologic stresses is the single most important property of bone from the clinical perspective. Prediction of biomechanical performance is potentially important in the military setting in order to match personnel with duty assignments that they can perform effectively with minimal risk of injury.

REFERENCES

1. Yershov, Y., T.H. Baldini, S. Villagomez, T. Young, M.L. Martin, R.S. Bockman, M.G. Peterson, and R.D. Blank, *Bone strength and related traits in HcB/Dem recombinant congenic mice.* J Bone Miner Res, 2001. **16**(6): p. 992-1003.
2. Blank, R.D., *Breaking down bone strength: a perspective on the future of skeletal genetics.* J Bone Miner Res, 2001. **16**(7): p. 1207-11.
3. Beamer, W.G., K.L. Shultz, L.R. Donahue, G.A. Churchill, S. Sen, J.R. Wergedal, D.J. Baylink, and C.J. Rosen, *Quantitative trait loci for femoral and lumbar vertebral bone mineral density in C57BL/6J and C3H/HeJ inbred strains of mice.* J Bone Miner Res, 2001. **16**: p. ???
4. Boskey, A.L., R.D. Blank, and S.B. Doty, *Vitamin C-sulfate inhibits mineralization in chondrocyte cultures: a caveat.* Matrix Biol, 2001. **20**(2): p. 99-106.

ELSEVIER

Matrix Biology 20 (2001) 99–106

MATRIX BIOLOGY

www.elsevier.com/locate/matbio

Vitamin C-sulfate inhibits mineralization in chondrocyte cultures: a caveat

Adele L. Boskey*, Robert D. Blank, Stephen B. Doty

Mineralized Tissues Research Section, Research Division, The Hospital for Special Surgery and Weill Medical College of Cornell University, 535 East 70th Street, New York, NY 10021, USA

Received 29 June 2000; received in revised form 21 December 2000; accepted 4 January 2001

Abstract

Differentiating chick limb-bud mesenchymal cell micro-mass cultures routinely mineralize in the presence of 10% fetal calf serum, antibiotics, 4 mM inorganic phosphate (or 2.5 mM β-glycerophosphate), 0.3 mg/ml glutamine and either 25 μg/ml vitamin C or 5–12 μg/ml vitamin C-sulfate. The failure of these cultures to produce a mineralized matrix (assessed by electron microscopy, ^{45}Ca uptake and Fourier transform infrared microscopy) led to the evaluation of each of these additives. We report here that the 'stable' vitamin C-sulfate (ascorbic acid-2-sulfate) causes increased sulfate incorporation into the cartilage matrix. Furthermore, the release of sulfate from the vitamin C derivative appears to be responsible for the inhibition of mineral deposition, as demonstrated in cultures with equimolar amounts of vitamin C and sodium sulfate.

Keywords: Ascorbic acid; Ascorbic-acid-2 sulfate; Vitamin C; Mineralization; Cell culture

1. Introduction

Ascorbic acid (vitamin C) is an obligatory requirement in cultures of differentiated osteoblasts (Dean et al., 1994; Franceschi et al., 1995; Siggelkow et al., 1999; Torii et al., 1996; Tullberg-Reinert and Jundt, 1999) and chondrocytes (Boskey et al., 1991b; Hall, 1981; Leboy et al., 1989; Shapiro et al., 1991; Sullivan et al., 1994; Venezian et al., 1998) where it is a co-factor for collagen hydroxylases (Tschank et al., 1994), an activator of alkaline phosphatase gene expression (Leboy et al., 1989; Venezian et al., 1998) and a stimulator of chondrocyte maturation (Leboy et al., 1997). Because vitamin C is rapidly oxidized to form toxic ascorbyl radicals (Makino et al., 1999) it must be prepared fresh before each charge of cell culture medium. Vitamin C persists in cultured tissues for approximately 24 h, although it is detectable in tissue culture medium for only 2 h (Roach et al., 1985). Addition of fresh vitamin C is not possible for cell culture experiments carried out in bioreactors on board the space shuttle or in biosatellites. To circumvent this problem, following preliminary evaluation, vitamin C-sulfate, a reportedly stable derivative of vitamin C (Machlin et al., 1976; Tolbert et al., 1975), was used in chondrocyte cultures flown on the several NASA shuttle missions (Doty et al., 1999). Recently, to save technician time, we replaced the addition of fresh vitamin C with vitamin C-sulfate for ground-based laboratory experiments. We report here that vitamin C-sulfate inhibits matrix mineralization of differentiating mesenchymal cell micro-mass cultures supplemented with inorganic phosphate or β-glycerophosphate, without having effects on cell viability, overall matrix synthesis, or alkaline phosphatase activity.

* Corresponding author. Tel.: +1-212-606-1453; fax: +1-212-472-5331.

E-mail address: boskeya@hss.edu (A.L. Boskey).

0945-053X/99/$ - see front matter
PII: S0945-053X(01)00116-0

2. Materials and methods

2.1. Cell culture methodology

Chick limb-bud mesenchymal cells were isolated from stage 21–24 (Hamburger and Hamilton, 1951) fertilized White Leghorn eggs (Truslow Farms, Chestertown, MD) as described in detail elsewhere (Boskey et al., 1992b). The eggs were maintained in a humidified incubator at 37°C for 4.5 days. The embryos were then sterilely withdrawn from the eggs and their limb buds removed into 0.9% USP grade saline (Abbott Laboratories, N Chicago, IL). Cells, released from the limb buds by digestion with 5 ml 0.25 wt.% trypsin-0.53 mM EDTA (GIBCO, Grand Island, NY), were separated from debris by passage through two layers of 20-μm Nitex membrane (Tetko Inc., Ardsley, NY). Cells were counted with a hemocytometer, checked for viability by trypan blue dye exclusion and pelleted in the cold at 2300 rev/min. In all cases, viability was greater than or equal to 97%. Cells were resuspended in medium containing 1.3 mM Ca and plated using the micro-mass technique (Ahrens et al., 1977), at a density of 0.75 million cells per 20 μl drop in 35 × 10 mm Falcon dishes and allowed to attach for 2 h in a humidified atmosphere of 5% CO_2 at 37°C. After 2 h, Dulbecco's modified essential medium (DMEM, GIBCO Formula 80-0303A, Grand Island, NY) which initially contained 1 mM inorganic phosphate and 0.3 mM calcium, was adjusted to have final concentrations of 1.3 mM calcium chloride, 1000 mg/l glucose and 50 units/ml penicillin and 25 μg/ml streptomycin, 10% fetal calf serum (GIBCO, Grand Island, NY) and 0.3 mg/ml glutamine. Mineralizing cultures were further supplemented with 3 mM inorganic phosphate from day 2 onward, making the total inorganic phosphate content 4 mM. In preparation for a NASA space flight, the cultures were maintained in a CellMax Quad artificial capillary cell culture system (Cellco, Inc., Germantown, MD), consisting of a chamber to contain cells flushed with medium at controlled temperatures and pressure. Medium containing 2.5 mM β-glycerophosphate was recycled through the chambers at a rate of 6 ml/min. Half of the chambers received 25 μg/ml vitamin C, prepared fresh with each medium change, with the medium bottles changed every 2 days. The other half received 5 μg/ml vitamin C-sulfate prepared once and recycled for the length of the experiment. Based on the results of that study (Fig. 1), vitamin C-sulfate was used for NASA experiments. For the purpose of the study reported here, the vitamin C supplements (described below) were added with every medium change from day 2. Non-mineralizing cultures received no phosphate supplements but did receive the ascorbate supplements. Medium was changed every 48 h. Cultures were maintained for 21 days with day 0 referring to the day of plating.

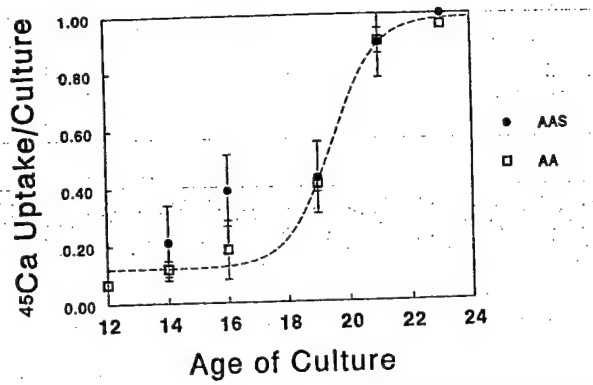

Fig. 1. ^{45}Ca uptake in differentiating chick-limb bud mesenchymal cell cultures, maintained in Cell-Max cartridges for 15 days, in the presence of recirculating medium with (open squares) 25 μg/ml (0.28 μM) vitamin C (AA) changed every 2 days, or (closed circles) 5 μg/ml vitamin C-sulfate (AAS, 0.05 μM). The dotted line is fitted to both sets of data. No significance differences were detected at any time point.

2.2. Vitamin C additives

Vitamin C [sodium ascorbate (Sigma Chemicals, St Louis, MO)], vitamin C-sulfate [sodium ascorbate-2-sulfate (Sigma Chemicals, St Louis, MO)] stored at −20°C as per manufacturers directions) or vitamin C plus an equal molar concentration of sodium sulfate (Fisher Chemicals, Springfield, NJ) were added to cultures in concentrations of 25, 12.5 or 5 μg/ml. Vitamin C was also added at a concentration of 50 μg/ml. To determine whether the Vitamin C-sulfate degraded 'on the shelf', in some experiments the reagent which was acquired in 1995 (old) and was still valid according to the manufacturer, was used, while in others the vitamin C-sulfate was used within 1 week of receipt from the manufacturer and prepared fresh with each change of medium (fresh). Another batch of cultures received this same vitamin C-sulfate prepared at the start of the experiment, but not remade for each change of medium (new). In another set of experiments, the 'new' reagent was heated at 60°C for 4 h to accelerate any breakdown. Cultures prepared from the same cell preparation but maintained with the different vitamin C sources were collected for analyses on days 5, 12, 16, 19 and 21. Cell viability and the ability to form chondrocyte nodules was determined on day 5, based on propidium iodide and alcian blue staining, respectively.

2.3. Matrix and cell parameters

Cell and matrix morphology and mineral localization were analyzed by transmission electron micro-

scopy (TEM). Samples were washed first with 0.05 M cacodylate buffer and then fixed in the culture dish for 12–18 h at 4°C in EM fixative (0.5% glutaraldehyde, 2% paraformaldehyde, 0.05 M pH 7.2 cacodylate buffer). After removal of the fixative, samples were stored at 4°C in 0.05 M cacodylate buffer containing 7% sucrose. Fixed cultures were removed from the dish, post-fixed with 2% aqueous osmium, dehydrated in a graded series of alcohols and embedded in Spurr's resin. Thin sections were collected on water containing bromthymol blue as an indicator for pH above 8.0 to prevent mineral dissolution. Sections stained with lead citrate and alcoholic uranyl acetate were examined on a Philips CM12 electron microscope and representative micrographs photographed for presentation.

Matrix properties in cultures treated with different supplements were measured on day 16. Specifically, total proteoglycan content was determined using a modification of the dimethylene blue staining method (Farndale et al., 1982), with relative values reported as absorbance at 595 nm. To determine the extent of proteoglycan sulfation, parallel dishes labeled at day 15 with $^{35}SO4$ (1 uCi/ml) for 16 h were subjected to the dimethylene blue staining procedure and the radiolabelled dimethylene blue-proteoglycan complex extracted into 4 M guanidine hydrochloride and an aliquot of the extract subjected to scintillation counting. Data was expressed as $^{35}SO_4$/proteoglycan absorbance. Collagen hydroxyproline was measured in 0.1-mg aliquots of lyophilized mineralizing day 16 cultures. Cultures were hydrolyzed in 6 N HCl in vacuo, after flushing with nitrogen, at 110°C for 24 h. An aliquot of each hydrolysate was then analyzed for hydroxyproline on a Varian HPLC 9012/9050 configured as an amino acid analyzer (AA911 column, Interaction) with ninhydrin color development at 135°C monitored at 440 nm (Uzawa et al., 1998). Data

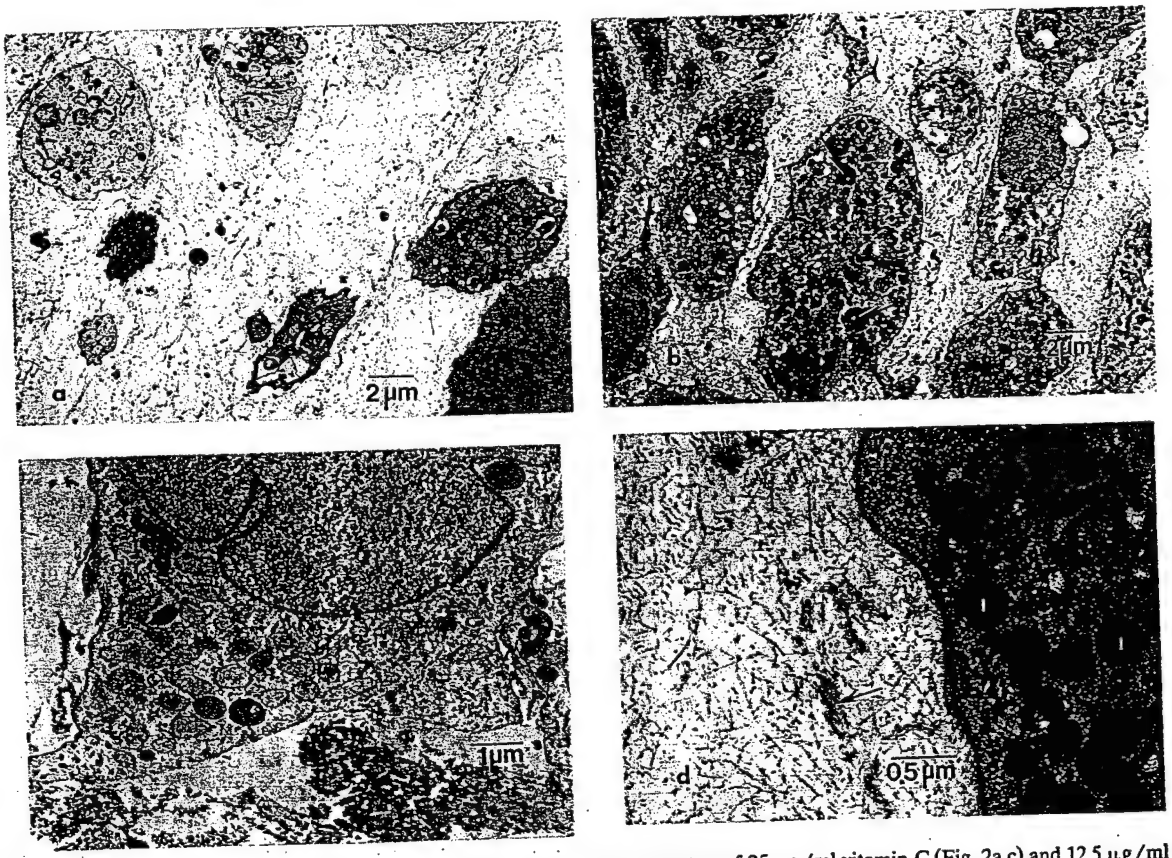

Fig. 2. Morphological differences between in vitro cartilage growth in the presence of 25 μg/ml vitamin C (Fig. 2a,c) and 12.5 μg/ml vitamin C-sulfate (Fig. 2b,d). Fig. 2a,b are control, non-mineralizing cultures and figures c and d are mineralizing cultures. (a) The typical appearance with vitamin C shows chondrocytes with normal cytology (i.e. endoplasmic reticulum (ER), golgi, mitochondria, etc.) and significant space between each cell which is filled with collagen fibers and proteoglycans. (b) These chondrocytes, grown in the presence of 12.5 μg/ml vitamin C-sulfate show membrane bound cytoplasmic inclusions (arrows) scattered among the normal cytoplasmic organelles. In addition, the cells are closely positioned to each other because of reduced matrix volume compared to the standard vitamin C treated cells shown in Fig. 2a. (c) Typical day 21 mineralizing culture with vitamin C. The mineral has completely covered the underlying collagen matrix. A calcific deposit has formed in the cartilage matrix adjacent to a chondrocyte with normal looking cytoplasmic content. (d) Mineralizing culture treated with vitamin C-sulfate. This, day 21, culture shows a small amount of electron dense material (arrows) deposited along some of the collagen fibers. Well-formed calcific deposits were not found. At this magnification, membrane bound cytoplasmic inclusions (I) within the chondrocytes are noted.

were expressed as nmoles hydroxyproline per mg dry culture weight.

Alkaline phosphatase activity (Sigma Test Kit 104-LL, Sigma Diagnostics, St Louis, MO) was monitored on day 12. The cultures were washed twice with 0.9% sodium chloride and digested at room temperature for 30 min in a buffer containing 0.15 M pH 9.0 Tris, 0.1 mM magnesium chloride, 0.1 mM zinc chloride and 1% Triton. The cultures were broken apart with a cell scraper and the incubation repeated and the activity of the total extract measured using *p*-nitrophenyl-phosphate as the substrate.

2.4. Mineral analyses

The accumulation of mineral in the cultures was assayed, as detailed elsewhere (Boskey et al., 1992b, 1996, 1997b) based on ^{45}Ca uptake (expressed per total culture). In brief, ^{45}Ca uptake was determined for each micromass culture spot, following hydrolysis of the spot in 2 N HCl (2 h, 60°C) and scintillation counting. Uptake was expressed as percentage of mineralizing control cultures at day 21. The presence of mineral was also validated by Fourier transform infrared microspectroscopy, FT-IR (Boskey et al., 1992a). FTIR imaging and microscopy studies were done on fresh cultures, placed and air dryed, on barium fluoride IR windows. Spectra were recorded at 20-μm resolution using a BioRad Infrared Spectrometer (Cambridge, MA) with an MCT detector.

2.5. Statistical evaluation

Each experiment was performed at least in triplicate, with three–four dishes of each condition for each time point for each individual experiments. In each independent experiment, the average for each condition at each time point was calculated and these average values used to calculate means for all experiments. Significant differences between experimental and control conditions were evaluated based on ANOVA and the appropriate statistical test. A $P \leq 0.05$ was taken as significant.

3. Results

Fig. 1 presents the ^{45}Ca uptake in the Cell-Max cartridges, comparing a typical culture with 5 μg/ml vitamin C-sulfate (made once) and 25 μg/ml vitamin C (prepared fresh every other day). As can be seen, there was no detectable difference.

Fig. 2 presents typical micrographs which indicate that the appearance of the cellular morphology and mineral deposition in cultures treated with 12.5 μg/ml vitamin C-sulfate differs from those treated with 25 μg/ml vitamin C. Although the appearance of the matrix seems normal in both non-mineralizing (Fig. 2a,b) and mineralizing cultures (Fig. 2c,d), in all micrographs examined, there was less matrix between chondrocytes following vitamin C-sulfate treatment (Fig. 2b,d) compared to vitamin C alone (Fig. 2a,c). Also, many of the chondrocytes showed inclusion bodies (Fig. 2d) suggesting that cell function is not completely normal after exposure to vitamin C-sulfate. The appearance of the collagen and proteoglycans, however, was not noticeably different.

The various vitamin C preparations also did not have a significant effect on nodule size (not shown), or on total proteoglycan content (Fig. 3a), however, $^{35}SO_4$ incorporation into the proteoglycans present was significantly increased in all cultures treated with vitamin C-sulfate (Fig. 3b). Furthermore, the extent of the increase was greater with the higher doses of vitamin C-sulfate. $^{35}SO_4$ uptake could not be measured in cultures treated with vitamin C and sodium sulfate, because of the relative concentrations of cold and radiolabelled sulfate. Alkaline phosphatase activity (Fig. 3c) was not altered by the various vitamin C treatments at day 12.

The hydroxyproline content of the matrix of the mineralizing cultures was slightly but not significantly reduced in cultures treated with vitamin C-sulfate as contrasted with cultures given vitamin C. The three concentrations of vitamin C used (12.5, 25 and 50 μg/ml) yielded the same hydroxyproline content and there was not a dose-dependent effect of vitamin C-sulfate (Fig. 4) on hydroxyproline content. The mineralizing matrices of the cultures treated with vitamin C-sulfate or vitamin C and sodium sulfate had a lower mass at day 16 (3.05 ± 0.38 mg) as contrasted to 5.08 ± 1.1 mg for the cultures treated with ascorbate ($P < 0.003$, Welch non-parametric *t*-test).

The failure to mineralize in the cultures given the sulfated form of vitamin C or vitamin C + Na_2SO_4 was evidenced by the decreased ^{45}Ca uptake (Fig. 5) as well as the absence of mineral in FT-IR spectra (not shown). The data in Fig. 5 show an average of the data for each of the concentrations tested, as the uptake in cultures with 5 or 12.5 μg/ml vitamin C-sulfate did not differ by more than 5% and the uptake in cultures with 12.5, 25 and 50 μg/ml vitamin C agreed to within 2%. Cultures given 'fresh' vitamin C-sulfate, from a new bottle and prepared with each medium change, were most similar to control cultures, but ^{45}Ca uptake was highly variable. Cultures which received the same ('new') vitamin-C sulfate solution, prepared only at the start of the experiment, showed a decrease in calcium accumulation. Cultures given the old vitamin C-sulfate, heated vitamin C-sulfate, or fresh vitamin C plus sodium sulfate showed no mineral accretion. Furthermore, ^{45}Ca uptake in

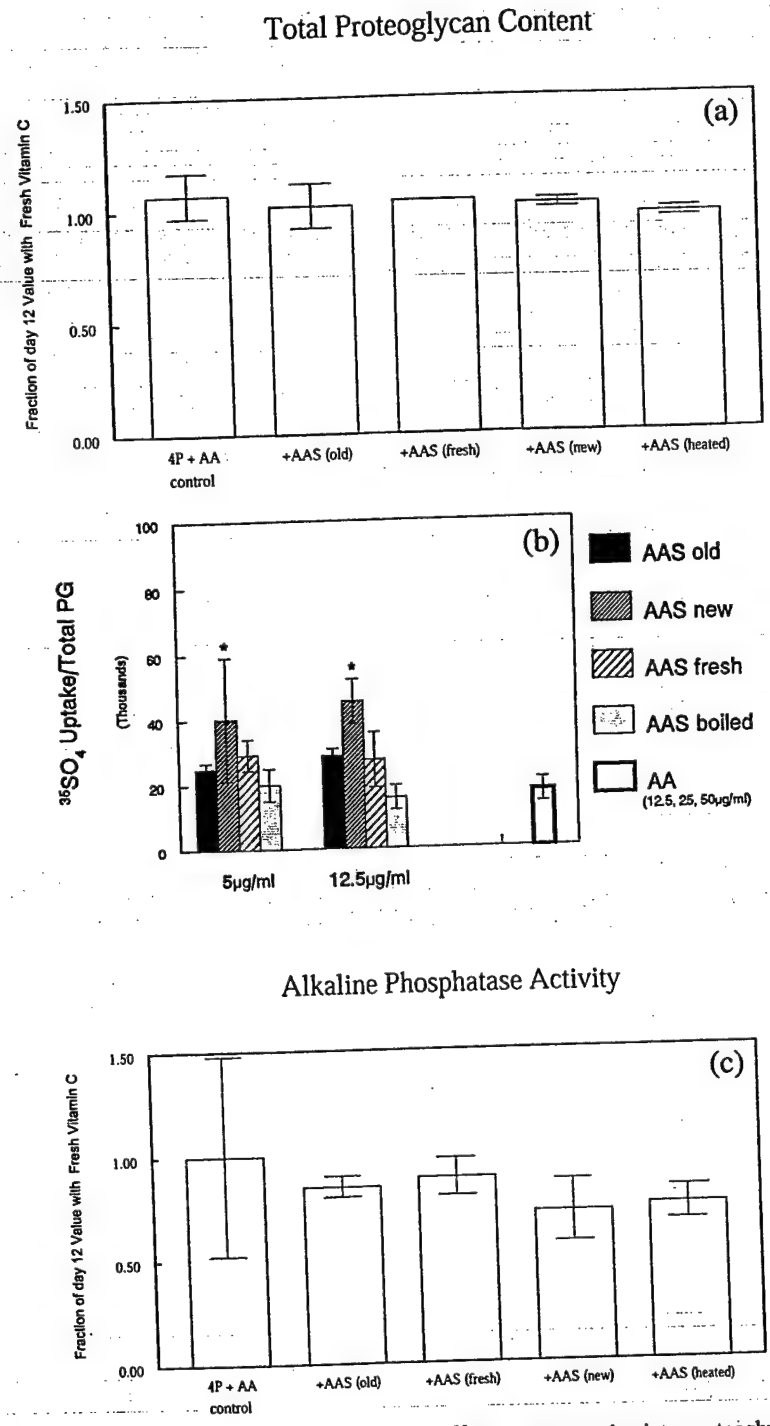

Fig. 3. Effect of vitamin C additives on (a) total proteoglycan content, (b) $^{35}SO_4$ incorporation into proteoglycans and (c) alkaline phosphatase activity, measured on day 12. Values are mean ± S.D. for $n = 3$ experiments. AA = vitamin C, AAS = vitamin C-sulfate.

the non-mineralizing vitamin C supplemented cultures was relatively constant, whereas, in the vitamin C-sulfate supplemented cultures, ^{45}Ca uptake increased 100% within 10 days and the rate of calcium uptake was 3 × that in the vitamin C treated cultures (data not shown).

4. Discussion

This study was not undertaken to investigate the mechanism of action of vitamin C as compared to vitamin C-sulfate, which has been described in detail elsewhere (Tolbert et al., 1975), but rather to de-

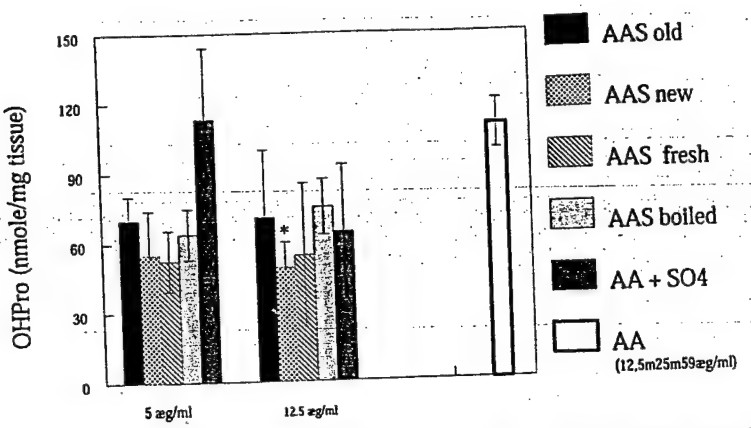

Fig. 4. Effect of vitamin C additives on hydroxyproline content of the culture matrix. Hydroxyproline content was measured on day 16 in mineralizing cultures supplemented with 5 or 12.5 μg/ml vitamin C-sulfate (AAS) from an old bottle (old), vitamin C-sulfate prepared with each medium change (fresh), vitamin C-sulfate from a new bottle, but not prepared fresh for each medium change (new), vitamin C-sulfate that was heated to promote breakdown (heated) and vitamin C with equimolar amounts of sodium sulfate ($AA + SO_4$). Freshly prepared vitamin C (AA) was used in concentrations of 12.5, 25 and 50 μg/ml and results are shown as mean for all concentrations ($n = 9$).

termine why cultures which had a reproducible pattern of mineral deposition for many years (e.g. Boskey et al., 1991b, 1992a,b, 1996, 1997b) stopped mineralizing when for the purpose of efficiency, our laboratory switched from using vitamin C to vitamin C-sulfate.

Our initial studies had shown vitamin C-sulfate at concentrations less than 12.5 μg/ml were not toxic in these cultures and that was confirmed here. Vitamin C-sulfate, which was not prepared fresh with each change of medium, however, or was not newly acquired from the manufacturer, inhibited mineralization. Since there is no advantage to using the sulfated form if it has to be prepared with each medium change, there appears to be no rationale for the use of this 'stable' form in this type of culture. A vitamin C-2-phosphate that does not form ascorbyl radicals is also available (Makino et al., 1999) and this stable vitamin C derivative has been used in several os-

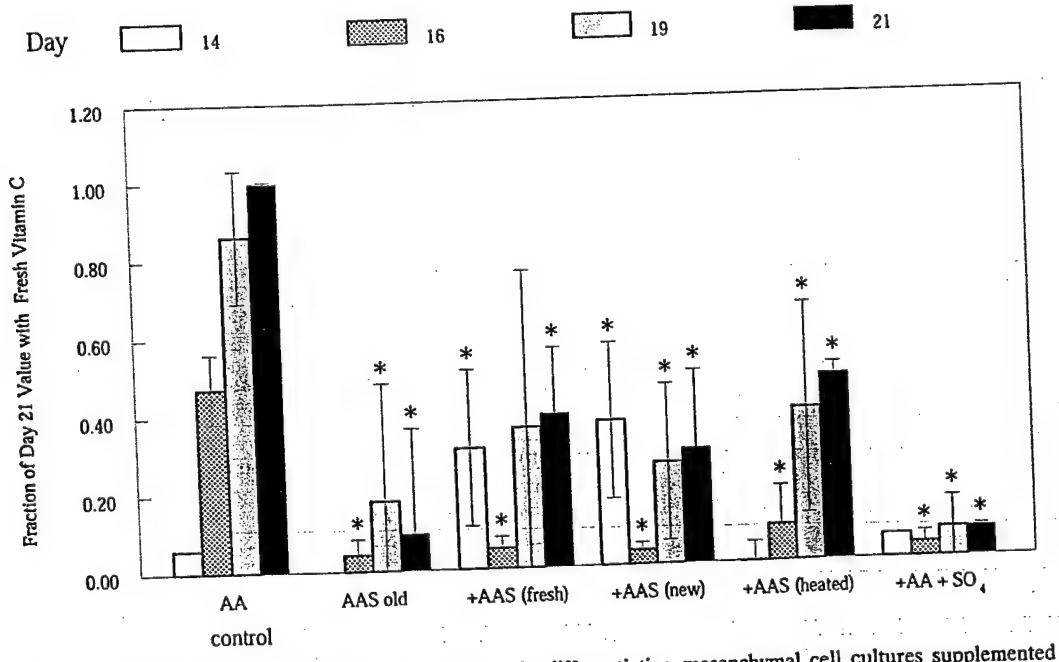

Fig. 5. Effect of vitamin C supplements on mineral accumulation in differentiating mesenchymal cell cultures supplemented with freshly prepared vitamin C (AA) in concentrations of 12.5, 25 and 50 μ/ml, or 5 or 12.5 μg/ml vitamin C-sulfate (AAS) from an old bottle (old), vitamin C-sulfate prepared with each medium change (fresh), vitamin C-sulfate from a new bottle, but not prepared fresh with each medium change (new), vitamin C-sulfate that was heated to promote breakdown (heated) and vitamin C with equimolar amounts of sodium sulfate ($AA + SO_4$). Absolute ^{45}Ca uptake has been normalized to uptake at 21 days in mineralizing cultures ($4P + AA$), values are mean ± S.D. for three–six cultures per time point. * Significantly different from same time point in mineralizing cultures with 25 μg/ml AA cultures, $P < 0.05$.

teoblast (Gronthos et al., 1994; Hitomi et al., 1992; Jaiswal et al., 1997; Tullberg-Reinert and Jundt, 1999; Torii et al., 1994) and other connective tissue and muscle (Fermor et al., 1998; Mitsumoto et al., 1994) culture systems. Although this phosphorylated-derivative might have been preferable in the mineralizing culture, it would have slightly increased local phosphate concentrations in the non-mineralizing controls which are very sensitive to changes in phosphate content (Boskey et al., 1992b) and thus we did not investigate its use.

There are several possible explanations for the observed effects of vitamin C-sulfate on development of a mineralized matrix. Vitamin C (ascorbic acid) is oxidized generating toxic ascorbyl radicals and peroxides (Wilgus and Roskoski, 1988) and we have previously shown in this system that high vitamin C doses cause demonstrable cell death (Boskey et al., 1991b). The vitamin C-sulfate concentrations used in our culture system, however, are far below this value. With the lower concentrations of vitamin C-sulfate used in these cultures, there was no EM evidence of cell death and the vitamin-C concentrations were 1/8 that previously shown to cause cell necrosis in this system. Thus, while viable cells are required for cartilage calcification (Boskey et al., 1996), the failure to mineralize does not appear to be due to cell death. The use of vitamin C-sulfate did slightly (but not significantly) decrease the extent of prolylhydroxylation, suggesting that collagen production was not extensively altered. The lack of significance may be related to the decreased weight of cultures treated with sulfated vitamin C, however, the ~40% difference in weight is most likely attributable to the presence of mineral in the vitamin C treated cultures and not to different amounts of collagen being present.

Vitamin C-sulfate is a substrate for sulfatases (Fluharty et al., 1976; Hatanaka and Egami, 1976; Roy, 1979) that are abundant in cartilage (Schwartz and Adamy, 1976) and most likely in this culture system. In cartilage, the proteins sulfated are most likely the proteoglycans, which are known inhibitors of calcification both in solution (Boskey, 1989; Boskey et al., 1997a), in animal models (Boskey et al., 1991a) and in this culture system (Boskey et al., 1997b). Total proteoglycan content was not decreased in the presence of vitamin C-sulfate, however, sulfate incorporation into total proteoglycans was significantly increased, suggesting that increased Ca-chelation by the over-sulfated proteoglycans is the major factor causing decreased mineralization.

Shapiro and Poon (1975) noted that the sulfate transfer from vitamin C-sulfate to chondroitin sulfate proteoglycans in chondrocyte cultures did not occur by direct transfer, but was accounted for by decomposition during storage at −20°C for several days. It is, therefore, likely that in the present study, the decomposition of the vitamin C-sulfate results in increased sulfation of proteoglycans (Brand et al., 1989; Silbert and DeLuca, 1969; van der Kraan et al., 1988), hence, the high ^{45}Ca uptake in the non-mineralizing controls, reflecting Ca chelation by the matrix. Calcium chelation by the more highly sulfated proteoglycans could contribute to the failure of those cultures to support mineralization. Because it is tempting to use a stable as contrasted with an unstable essential additive, it is important to consider the consequences of a seemingly innocuous medium supplement such as vitamin C-sulfate on culture behavior.

Acknowledgements

Supported by NIH grant AR037661. The authors would like to thank Ms Dalina Stiner, Ms Orla O'Shea and Mr Anthony Labissiere for their technical assistance. IR imaging was performed in the IR Imaging Core and histologic evaluation was done in the Analytical Microscopy Core, both components of the Musculoskeletal Core Center at the Hospital for Special Surgery (AR 46121). The authors appreciate the assistance of Dr Mitsui Yamauchi with the HPLC analysis of hydroxyproline.

References

Ahrens, P.B.A., Solursh, M., Reiter, R.S., 1977. Stage related capacity for limb chondrogenesis in cell culture. Dev. Biol. 60, 69–82.

Boskey, A.L., 1989. Hydroxyapatite formation in a dynamic gel system: Effects of type I collagen, lipids, and proteoglycans. J. Phys. Chem. 93, 1628–1633.

Boskey, A.L., Doty, S.B., Stiner, D., Binderman, I., 1996. Viable cells are a requirement for in vitro cartilage calcification. Calcif. Tissue Int. 58, 177–185.

Boskey, A.L., Maresca, M., Hjerpe, A.., 1991a. Hydroxyapatite formation in the presence of proteoglycans of reduced sulfate content: studies in the brachymorphic mouse. Calcif. Tissue Int. 49, 389–393.

Boskey, A.L., Stiner, D., Doty, S., Binderman, I., 1991b. Requirement of vitamin C for cartilage calcification in a differentiating chick limb-bud mesenchymal cell culture. Bone. 12, 277–282.

Boskey, A.L., Pleshko, N., Mendelsohn, R., Doty, S.B., Binderman, I., 1992a. FT-IR microscopic mappings of early mineralization in chick limb bud mesenchymal cell cultures. Calcif. Tissue Int. 51, 443–448.

Boskey, A.L., Spevak, M., Doty, S., Rosenberg, L., 1997a. Effects of bone proteoglycans, decorin and biglycan on hydroxyapatite formation in a gelatin gel. Calcif. Tissue Int. 61, 298–305.

Boskey, A.L., Stiner, D., Binderman, I., Doty, S.B., 1997b. Effects of proteoglycan modification on mineral formation in a differentiating chick limb-bud mesenchymal cell culture system. J Cell Biochem. 64, 632–643.

Boskey, A.L., Stiner, D., Leboy, P., Doty, S., Binderman, I., 1992b. Optimal conditions for cartilage calcification in differentiating chick limb-bud mesenchymal cells. Bone Mineral 16, 11–37.

Brand, H.S., van Kampen, G.P., van de Stadt, R.J., Kuijer, R., van der Korst, J.K., 1989. Effect of sulfate concentration on gly-

cosaminoglycan synthesis in explant cultures of bovine articular cartilage. Cell. Biol. Int. Rep. 13, 153–162.
Dean, D.D., Schwartz, Z., Bonewald, L. et al., 1994. Matrix vesicles produced by osteoblast-like cells in culture become significantly enriched in proteoglycan-degrading metalloproteinases after addition of beta-glycerophosphate and ascorbic acid. Calcif. Tissue Int. 54, 399–408.
Doty, S.B., Stiner, D., Telford, W., 1999. The effect of spaceflight on cartilage cell cycle and differentiation. J. Gravit. Physiol. 6, 89–90.
Farndale, R.W., Sayers, C.A., Barrett, A.J., 1982. A direct spectrophotometric microassay for sulfated glycosaminoglycans in cartilage cultures. Connect. Tissue Res. 9, 247–248.
Fermor, B., Urban, J., Murray, D., Pocock, A., Lim, E., Francis, M., Gage, J., 1998. Proliferation and collagen synthesis of human anterior cruciate ligament cells in vitro: effects of ascorbate-2-phosphate, dexamethasone and oxygen tension. Cell Biol. Int. 22, 635–640.
Fluharty, A.L., Stevens, R.L., Miller, R.T., Shapiro, S.S., Kihara, H., 1976. Ascorbic acid-2-sulfate sulfhohydrolase activity of human arylsulfatase A. Biochim. Biophys. Acta 429, 508–516.
Franceschi, R.T., Wilson, J.X., Dixon, S.J., 1995. Requirement for Na(+)-dependent ascorbic acid transport in osteoblast function. Am. J. Physiol. 268, C1430–A1439.
Gronthos, S., Graves, S.E., Ohta, S., Simmons, P.J., 1994. The STRO-1 + fraction of adult human bone marrow contains the osteogenic precursors. Blood. 84, 4164–4173.
Hall, B.K., 1981. Modulation of chondrocyte activity in vitro in response to ascorbic acid. Acta Anat. (Basel) 109, 51–63.
Hamburger, V., Hamilton, H.L., 1951. A series of normal stages in the development of the chick embryo. J. Morphol. 88, 49–92.
Hatanaka, H., Egami, F., 1976. Sulfate incorporation from ascorbate 2-sulfate into chondroitin sulfate by embryonic chick cartilage epiphysis. J. Biochem. 80, 1215–1221.
Hitomi, K., Torii, Y., Tsukagoshi, N., 1992. Increase in the activity of alkaline phosphatase by L-ascorbic acid 2-phosphate in a human osteoblast cell line, HuO-3N1. J. Nutr. Sci. Vitaminol. 38, 535–544 (Tokyo).
Jaiswal, N., Haynesworth, S.E., Caplan, A.I., Bruder, S.P.., 1997. Osteogenic differentiation of purified, culture-expanded human mesenchymal stem cells in vitro. J Cell Biochem. 64, 295–312.
Leboy, P.S., Sullivan, T.A., Noorayayazdun, M., Venezian, R.A., 1997. Rapid chondrocyte maturation by serum-free culture with BMP-2 and ascoribic acid. J Cell Biochem. 66, 394–403.
Leboy, P.S., Vaias, L., Uschmann, B., Golub, E., Adams, S.L., Pacifici, M., 1989. Ascorbic acid induces alkaline phosphatase, type X collagen and calcium deposition in cultured chick chondrocytes. J. Biol. Chem. 264, 17281–17586.
Machlin, L.J., Garcia, F., Kuenzig, W., Richter, C.B., Spiegel, H.E., Brin, M., 1976. Lack of antiscorbutic activity of ascorbate 2-sulfate in the rhesus monkey. Am. J. Clin. Nutr. 29, 825–831.
Makino, Y., Sakagani, H., Takeda, M., 1999. Induction of cell death by ascorbic acid derivatives in human renal carcinoma and glioblastoma cell lines. Anticancer Res. 19, 3125–3132.
Mitsumoto, Y., Liu, Z., Klip, A., 1994. A long-lasting vitamin C derivative, ascorbic acid 2-phosphate, increases myogenin gene expression and promotes differentiation in L6 muscle cells. Biochem. Biophys. Res. Commun. 199, 394–402.
Roach, H.I., Hillier, K., Shearer, J.R., 1985. Stability of ascorbic acid and uptake of the vitamin by embryonic chick femurs during long-term culture. Biochim. Biophys. Acta 842, 133–138.
Roy, A.B., 1979. The hydrolysis of ascorbate 2-sulfate by sulfatase A. Methods Enzymol. 62, 42–47.
Schwartz, E.R., Adamy, L., 1976. Effect of ascorbic acid on arylsulfatase A and B activities in human chondrocyte cultures. Connect. Tissue Res. 4, 211–218.
Shapiro, I.M., Leboy, P.S., Tokuoka, T., Forbes, E., DeBolt, K., Adams, S.L., Pacifici, M., 1991. Ascorbic acid regulates multiple metabolic activities of cartilage cells. Am. J. Clin. Nutr. 54, 1209S–1213S.
Shapiro, S.S., Poon, J.P., 1975. Apparent sulfation of glycosaminoglycans by ascorbic acid 2-[3 5-S] sulfate: an explanation. Biochim. Biophys. Acta 385, 22–29.
Siggelkow, H., Rebenstorff, K., Kurre, W., Niedhart, C., Engel, I., Schulz, H., Atkinson, M.J., Hufner, M., 1999. Development of the osteoblast phenotype in primary human osteoblasts in culture: comparison with rat calvarial cells in osteoblast differentiation. J. Cell Biochem. 75, 22–35.
Silbert, J.E., DeLuca, S., 1969. Biosynthesis of chondroitin sulfate. (3) Formation of a sulfated glycosaminoglycan with a microsomal preparation from chick embryo cartilage. J. Biol. Chem. 244, 876–881.
Sullivan, T.A., Uschmann, B., Hough, R., Leboy, P.S., 1994. Ascorbate modulation of chondrocyte gene expression is independent of its role in collagen secretion. J. Biol. Chem. 269, 22500–22506.
Tolbert, B.M., Downing, M., Carlson, R.W., Knight, M.K., Baker, E.M., 1975. Chemistry and metabolism of ascorbic acid and ascorbate sulfate. Ann. N.Y. Acad. Sci. 258, 48–69.
Torii, Y., Hitomi, K., Tsukagoshi, N., 1996. Synergistic effect of BMP-2 and ascorbate on the phenotypic expression of osteoblastic MC3T3-E1 cells. Mol. Cell. Biochem. 165, 25–29.
Torii, Y., Hitomi, K., Tsukagoshi, N., 1994. L-ascorbic acid 2-phosphate promotes osteoblastic differentiation of MC3T3-E1 mediated by accumulation of type I collagen. J. Nutr. Sci. Vitaminol. 40, 229–238 (Tokyo).
Tschank, G., Sanders, J., Baringhaus, K.H., Dallacker, F., Kivirikko, K.V., Gunzler, V., 1994. Structural requirements for the utilization of ascorbate analogues in the prolyl 4-hydroxylase reaction. Biochem. J. 300, 75–79.
Tullberg-Reinert, H., Jundt, G., 1999. In situ measurement of collagen synthesis by human bone cells with a sirius red-based colorimetric microassay: effects of transforming growth factor beta2 and ascorbic acid 2-phosphate. Histochem. Cell Biol. 112, 271–276.
Uzawa, K, Marshall, M.K., Katz, E.P., Tanzawa, H., Yeowell, H.N., Yamauchi, M., 1998. Altered post-translational modifications of collagen in keloid. Biochem. Biophys. Res. Commun. 249, 652–655.
van der Kraan, P.M., Vitters, E.L., de Vries, B.J., van den Berg, W.B., van de Putte, L.B., 1988. Synthesis of aberrant glycosaminoglycans during cartilage culture in 'sulfate free' medium. J. Biochem. Biophys. Methods. 15, 273–277.
Venezian, R., Shenker, B.J., Datar, S., Leboy, P.S., 1998. Modulation of chondrocyte proliferation by ascorbic acid and BMP-2. J. Cell. Physiol. 174, 331–341.
Wilgus, H., Roskoski Jr., R., 1988. Inactivation of tyrosine hydroxylase activity by ascorbate in vitro and in rat PC12 cells. J. Neurochem. 51, 1232–1239.

DRAFT

Collagen Cross-Link Maturity and Crystallinity Indices Differ Markedly in Recombinant Congenic Mice Having Divergent Calculated Tissue Strength

Robert D. Blank

Michael Kaufman

Todd Baldini

Stephanie Bailey

Rajarsi Gupta

Yevgeniy Yershov

Adele L. Boskey

Susan N. Coppersmith

Richard S. Bockman

Peter Demant

Eleftherios P. Paschalis

ABSTRACT

The structural strength of a bone can be partitioned into architectural and material components. In 3-point bending tests of 6 month old female humeri from the HcB/Dem recombinant congenic series, 2 strains differed markedly in calculated failure stress as summarized in the table. We used Fourier Transform Infrared Spectroscopic Imaging (FTIRI) to determine whether differences in collagen cross-link maturity, crystallinity, or spatial ordering could account for the large difference in calculated tissue strength between these 2 strains with similar mineral content. Cross-link maturity and crystallinity were assayed as the absorbance ratios at 1660:1690 cm^{-1} and 1030:1020 cm^{-1}, respectively. One-dimensional spatial correlation functions were estimated to compare the uniformity of the indices within fields. For HcB/8, the mean cross-link maturity index is 1.654 and the median is 1.641. The mean and median HcB/23 cross-link maturity indices are 1.273 and 1.365, respectively. The difference in cross link maturity is highly significant ($\chi^2 = 1968$, 9 df, $P < 10^{-15}$). For HcB/8, the mean and median crystallinity index are 0.950 and 0.974, respectively. In HcB/23, the corresponding values are 0.840 and 0.909. As for cross link maturity, the difference between the strains is highly significant ($\chi^2 = 400$, 6 df, $P < 10^{-15}$). Cross-link maturity and crystallinity are highly and similarly correlated in both strains, with correlation coeffecients of 0.751 for HcB/8 and 0.758 for HcB/23 ($P < 10^{-16}$ in both strains). We did not find evidence of significant differences between the strains' 1-dimensional spatial correlation functions. The high correlation between cross-link maturity and crystallinity reflects the interdependence of the protein and mineral elements of bone matrix. The data illustrate the usefulness of FTIRI to examine bone quality and relate it to biomechanical performance.

INTRODUCTION

Fracture is the most significant clinical measure of bone's biomechanical performance. Epidemiologically, several types of fracture are recognized as "osteoporotic," occurring in the setting of minimal trauma. However, it is known that bone mineral density (BMD), while a useful clinical predictor of fracture risk, does not fully account for individual differences in fracture risk [1-6].

Biomechanical testing of bones harvested from experimental organisms is one approach by which the various contributors to bone strength can be studied [7, 8]. By loading bones according to contrived but reproducible protocols, such tests are capable of distinguishing strain-specific differences in mechanical performance. Moreover, it is well-established that the structural strength of a whole bone can be partitioned into architectural and material components. The bone's architecture takes into account the bone's size and shape, while the bone's material reflects the underlying strength of the tissue.

Recently, there has been growing interest in understanding the contributions of both the architectural and the material aspects of bone strength. Architectural investigations have included human studies of hip axis length (e.g. [9-15]), femoral neck bone distribution (e.g. [16, 17]), crumpling ratio (e.g. [18]), sexual dimorphism of bone modeling (e.g. [19-22]), and trabecular connectivity (e.g. [23-26]). In addition, in animal models there has been explicit use of anatomical measurements in the interpretation of biomechanical studies (e.g. [27-30]). Investigation of bone material strength have historically relied upon biochemical and biophysical methods, and have included quantitation of various protein and mineral components of bone tissue through a variety of technical approaches, including Fourier Transform Infrared spectroscopy (FTIR). By coupling FTIR detection to a microscope or to an array of microscopic

detectors, spectral analysis can be carried out on thin histologic preparations of bone, allowing the material properties of bone to be investigated on scales as small as 7 μm [31, 32]. These methods allow investigation of the role, if any, the microscopic organization of bone tissue plays in determining its material strength.

In this report, we extend previous observations of biomechanical performance in HcB/Dem recombinant congenic mice. In these experiments, we determined that the calculated tissue strength of bone in strains HcB/8 and HcB/23 differ greatly, in spite of similar mineral content. Here, we extend characterization of these strains to include FTIR imaging data from cortical bone samples. We find that the strains differ markedly in collagen cross link maturity and hydroxyapatite crystallinity. We also find that these 2 indices are highly correlated. We find no difference in the one-dimensional spatial correlation of either cross-link maturity or crystallinity parallel to the bone surface. These data are considered with regard to the mechanistic basis of bone strength.

MATERIALS AND METHODS

Mice: The HcB/Dem strains were established and are maintained at the Netherlands Cancer Institute. Briefly, the HcB/Dem mice are inbred strains derived from arbitrary pairs of N3 backcross animals [33-35]. The HcB/Dem strains have been genotyped at 130 marker loci distributed over each of the autosomes [36, 37]. Because they are inbred, individuals from a single strain have the same genetic composition, save for new mutations and residual unfixed chromosome segments [38, 39]. Less than 5% of the genome was unfixed at the time of genotyping; residual heterozygosity is expected to be reduced by half in each generation of inbreeding. The mice described in this report were maintained at the Hospital for Special Surgery until 6 to 7 months of age under 12 hour light-dark cycling and fed irradiated PICO 5058 rodent chow and autoclaved tap water ad lib. Only females were studied, because inclusion of males would have introduced sex-dependent variability in the traits in addition to the strain-specific and environmental variability already encountered. At sacrifice, body mass and rostro-anal length were measured. This work satisfied The Hospital for Special Surgery's requirements for the ethical use of laboratory research animals.

Ash Percentage: Bone mineral fraction was calculated by comparison of dry, defatted bone weight to ash weight of homogenized tissue [40, 41]. We chose to use entire bones rather than bones from which the epiphyses and marrow have been removed because the former technique is more reproducible in our hands.

Radiographic Analysis: Image analysis of fine focus contact radiographs of dissected humeri was performed as described and used to calculate CSA and I [41]. Humeral length was defined as the distance along the diaphysis from the trochlea to the humeral head's most distant point. Outer and inner diameters were measured in orthogonal projections just distal to the deltoid

tuberosity, perpendicular to the diaphyseal axis. CSA was calculated according to the elliptical approximation

$$CSA = \pi(ML\ OR * AP\ OR - ML\ IR * AP\ IR)$$

where OR is the outer and IR the inner radius in either the mediolateral (ML) or anteroposterior (AP) projection. *I* was also calculated according to the elliptical approximation [8]

$$I = \pi/4[(ML\ OR)^3(AP\ OR) - (ML\ IR)^3(AP\ IR)]$$

Image analysis was performed with SigmaScan (Jandel Scientific) image analysis software. All radiographs included stepped aluminum densitometric phantoms. Radiographic images were digitized with a Kodak digital camera, with the photographic field including a length scale.

Biomechanical Testing: Quasi-static 3 Point Bend Testing was performed on left humeri using posts designed and machined in-house with the MTS apparatus and Instron electronics as described [42, 43]. Humeri were oriented with the deltoid tuberosity downward and the specimens oriented with the central post adjacent to the distal end of the deltoid tuberosity. This orientation corresponds to the ML axis being parallel to the applied force. Posts were separated by 3.75 mm.

Biomechanical data were analyzed following several important assumptions. First, we assumed that bone strength is determined entirely by the cortical bone in the mid-diaphysis. Second, we assumed that the humeral diaphysis is an ellipse with its major axis lying in the ML plane and its minor axis lying in the AP axis. Calculated biomechanical parameters were obtained according to the following standard formulas for 3 point-bending of ellipses [8]:

Stress (σ), (MPa) = $FLc/4I$ with F= force, L = length, c = ML OR

Strain (ε), (mm/mm) = $12cd/L^2$ with c = ML OR, d = displacement, L = length

Young's Modulus (E), (MPa) = $(F/d)(L^3/48I)$

FTIR Imaging: The left tibia from 1 mouse of each strain was fixed in buffered formalin, dehydrated in ethanol, and embedded in PMMA, from which 3 μm mid-sagittal sections were obtained for FTIR imaging. FTIR imaging was performed using a BioRad Stingray FTIR imaging system, with automated subtraction of water vapor and PMMA spectra as previously described [44, 45]. In each analyzed field, pixels in which either the 1660:1690 cm^{-1} ratio fell outside of the 0 to 2.5 range or the 1030:1020 cm^{-1} ratio fell outside the 0 to 2.0 range were censored as bad data.

Statistical Analysis: Most statistical analyses were performed using SigmaStat 2.03 (Jandel Scientific) and the remainder were performed with Origin version 5.0 (Microcal). Student's t-test was used to compare HcB/8 and HcB/23 mice for anatomic features and biomechanical performance, with values for failure stress log-transformed prior to analysis to satisfy the test assumption of normality. Significance levels were Bonferroni-corrected to account for multiple comparisons. Interstrain comparisons of cross link maturity and crystallinity indices were done by χ^2 contingency table, taking the weighted average number of pixels in each 0.25 unit interval of the distribution for each strain. The Kolmogorov-Smirnov test was used to assess normality of the FTIR imaging data. Correlation between cross link maturity and crystallinity was performed on pooled data from all the scans, as this is a property of individual spectra, not of individual animals or scans. One-dimensional spatial correlation functions (1DCs) were calculated parallel to the bone surface according to the formula $g(r) = \Sigma(x_I - \ast)(x_{I+r} - \ast)/\sqrt{\Sigma}\ x_I - \ast)^2\sqrt{\Sigma(x_{I+r} - \ast)^2}$ where x_I is the index at a given pixel i, x_{I+r} is the index at a pixel located at a pixel r pixels from i, and $\ast$ is the average value of the index in the entire field. We calculated g(r) for $0 < r < 64$, omitting bad pixels and truncating r at the edge of the scanned field. To compare the correlation functions of the two strains, we hypothesized that the correlation

coefficient would decay over differing correlation lengths in the 2 strains. To test the hypothesis, a straight-line fit was made over the linear, small r region of g(r). The slopes of the fits for the samples were pooled for each strain and subjected to a t-test.

RESULTS

Calculated tissue strength differs between HcB/8 and HcB/23: We examined 9 6 month old female HcB/8 and 9 6 month old female HcB/23 mice. The anatomic and biomechanical properties of the animals is summarized in **table 1**. These data show that while humeral failure load and structural stiffness is similar in the 2 strains, HcB/23 achieves this strength through more favorable bone architecture and less favorable bone tissue strength, while HcB/8 does so through less favorable bone architecture and more favorable bone tissue strength. The inferiority of HcB/23 bone tissue strength is not due to lesser mineralization, as this strain has a greater ash percentage than HcB/8. These observations prompted us to use FTIR imaging to explore the possible basis for the marked difference in bone tissue strength between the strains, examining 4 400 μm^2 sections of bone from each strain.

Cross link maturity differs between HcB/8 and HcB/23: The ratio of absorbances at 1660 cm^{-1} and 1690 cm^{-1} is an index of the oxidation state of collagen cross links, with higher ratios indicating a greater proportion of pyridinoline relative to DHLNL [45]. Representative sections from each strain are shown in **figure 1**. Overall, the difference in cross link maturity is highly significant ($\chi^2 = 1968$, 9 degrees of freedom, $P < 10^{-15}$). The mean and median HcB/23 cross link maturity indices are 1.273 and 1.365, respectively. For HcB/8, the mean cross link maturity index is 1.654 and the median is 1.641. Neither of the distributions is normal, with $P < 10^{-15}$ for the Kolmogorov-Smirnov test of normality in both cases. The HcB/23 distribution is more negatively skewed than the HcB/8 distribution, with values of -1.727 and -0.185, respectively. The HcB/23 distribution has a kurtosis of 3.012 and the HcB/8 distribution has a kurtosis of 1.198. Thus, in addition to having different degrees of cross link oxidation, the distributions are shaped differently.

Crystallinity differs between HcB/8 and HcB/23: The ratio of absorbances at 1030 cm^{-1} and 1020 cm^{-1} is a composite index of the hydroxyapatite crystal size and perfection, with higher ratios indicating greater crystallinity. The crystallinity maps of the 2 strains are compared in **figure 2**. As for cross link maturity, the difference between the strains is highly significant ($\chi^2 =$ 400, 6 degrees of freedom, $P < 10^{-15}$). Also as for cross link maturity, the crystallinity distributions deviate markedly from normality ($P < 10^{-15}$ in both cases). The mean and median of the crystallinity index in HcB/23 are 0.840 and 0.909, respectively. For HcB/8, the corresponding values are 0.950 and 0.974. As for the cross link maturity distributions, the HcB/23 crystallinity distribution is more negatively skewed (-1.408 and –0.913) and more kurtotic (1.855 and 0.882) than the HcB/8 distribution. However, the crystallinity distributions are less dissimilar than the cross link distributions.

Cross link maturity and crystallinity are highly correlated: Because of the well-established relationship between the protein and mineral components of bone's extracellular matrix, we examined the pixel by pixel correlation of the collagen cross link maturity index and the crystallinity index. These properties were highly and similarly correlated in both strains, with correlation coeffecients of 0.751 for HcB/8 and 0.758 for HcB/23. In both strains, the results are highly significant ($P < 10^{-16}$).

Cross-link maturity and crystallinity are r similarly uniform in HcB/23 than in HcB/8: The FTIR imaging data summarized above consider pixels collectively, without regard for their spatial arrangement within the cortical bone. In order to explore whether the similarity of closely spaced pixels differs between strains, we investigated 1-dimensional spatial correlations in each of the FTIR samples. **Figure 3** shows the relationship between distance parallel to the bone surface in pixels and g(r), the correlation of the collagen cross link maturity index at 2 points

separated by distance r. Inspection of the figure shows that for small r, the decay of g(r) is linear and similar in the 2 strains. This relationship holds up to a pixel separation of approximately 10 pixels, corresponding to a distance of 70 μm. At larger r values, g(r) varies erratically. Similar results (not shown) were observed for the crystallinity index. Overall, the correlation functions of the 2 strains did not differ statistically. These data suggest that there is no difference in the short-range ordering of collagen cross-link maturity or crystallinity between the 2 strains. Further, these experiments provided no evidence of ordering over longer length scales.

DISCUSSION

In our initial survey of bone properties of the HcB/Dem recombinant congenic strains, we noted that HcB/8 and HcB/23 are similar with respect to failure load and ash percentage, but that HcB/23 has much inferior calculated tissue strength relative to HcB/8. While this difference is not as great as that between the parental strains C3H/DiSnA and C57BL/10ScSnA, the parental strains differ significantly in ash percentage as well [46]. These observations led us to explore the possibility that material properties amenable to investigation by FTIR imaging might provide insight into the dramatic difference in failure stress between the strains.

Collagen cross link maturity is one such property. Following collagen synthesis and secretion, individual collagen monomers are enzymatically cross linked in the extracellular space. In bone, the predominant covalent cross links between type 1 collagen molecules are formed by condensation of hydroxylysine and, to a lesser extent, lysine residues. Initial cross links are bimolecular and reducible, and these then mature to form pyridinoline and deoxypyridinoline by further condensation of either hydroxylysine or lysine, respectively. We previously showed that the 1660 cm^{-1}:1690 cm^{-1} absorbance ratio reflects the relative amounts of nonreducible pyridinoline cross links to reducible DHLNL cross links [45]. Cross links confer tensile strength and viscoelasticity on bone matrix, properties that improve fracture resistance in bending.

Hydroxyapatite crystallinity is a second such property. Crystallinity, as reflected by the 1030 cm^{-1}:1020 cm^{-1} absorbance ratio, reflects the size and perfection of the hydroxyapatite crystals [47]. The mineral component of bone matrix is a poorly crystalline and highly substituted, a property that facilitates exchange of bone and blood calcium and phosphate levels and thus contributing to bone's metabolic function as a reservoir for calcium. Our data suggest

that increased crystallinity improves mechanical performance. That distinct crystallinity optima for mechanical performance and mineral homeostasis exist is a hypothesis that warrants further study.

We report a high point-by-point correlation between cross link maturity and crystallinity indices. It is well-established that bone mineralization depends on and follows organic matrix synthesis temporally. In osteogenesis imperfecta, for example, defective type I collagen is the underlying problem, but BMC is generally low as well. Meunier and colleagues (e.g. [48, 49]) have used histologic methods to follow the progress of mineralization in osteonal bone. They found that mineralization occurs in 2 phases, an initial, relatively rapid initial phase followed by a subsequent slower continued mineral accretion. It is tempting to speculate that these observations are in fact illustrations of a more general, possibly mechanistic, relationship between cross link maturity and crystallinity.

There are important limitations to the work presented here. First, the mechanical test performed, 3-point bending, measures whole bone strength, not tissue strength. Tissue strength is calculated from the structural strength, bone dimensions measured from orthogonal plain radiographs, and a relatively crude simplifying assumption regarding the shape of the murine humeral diaphysis. These assumptions lead to important uncertainties regarding the failure stress and modulus estimates reported here. These technical limitations apply equally to the mechanical testing of both strains, and should therefore not affect the magnitude of the difference between the calculated failure stress and modulus between them. Moreover, 3-point bend testing is a contrived experimental fracture model and may differ mechanistically from clinical fracture. Second, the FTIR imaging was limited to single animals of each strain. While the number of individual spectra analyzed is large, interpretation must be cautious as the animals

tested might not be representative of their respective strains. Third, we used tibiae for FTIR imaging, but humeri for mechanical testing. Fourth, we examined formalin-fixed specimens, while subsequent work has demonstrated that this treatment tends to increase the cross link maturity index and decrease the crystallinity index relative to unfixed specimens [50]. As for the technical limitations of the mechanical testing, this limitation should not affect the difference between the strains.

These limitations notwithstanding, the data presented here provide evidence that differences in cross link maturity and crystallinity reflect differences in biomechanical performance not only in the presence of significant pathology (e.g. [51-54]), but also among strains of wild type mice. Turner and colleagues [29] also found evidence suggesting marked differences in tissue strength among the B X H recombinant inbred strains, but have not yet provided a mechanistic hypothesis regarding the origin of these differences. A fuller understanding of the role of these and other non-BMC components of bone tissue strength will no doubt help explain the apparent disparities between fracture reduction and changes in BMC in human clinical trials as well.

ACKNOWLEDGMENTS

RDB gratefully acknowledges support provided by DAMD17-00-1-0071. The US Army Medical Research Acquisition Activity, Ft. Detrick, MD, is the awarding and administering acquisition office. The views expressed do not necessarily reflect the position or policy of the US government, and no official endorsement should be inferred.

This work was supported in part from a grant to the University of Wisconsin under the Howard Hughes Medical Institute Research Resources Program for Medical Schools.

TABLES

Table 1. Anatomic and Biomechanical Properties of HcB/8 and HcB/23 Mice

Trait	HcB/8 (N=10)	HcB/23 (N=9)	P value
Body Mass (g)	19.9 ± 1.5	23.5 ± 1.1	$< 10^{-4}$
BMI (g/cm^2)	0.27 ± 0.01	0.25 ± 0.01	0.001
Humeral Length (mm)	11.1 ± 0.3	11.3 ± 0.2	NS
ML OD (mm)	1.07 ± 0.07	1.23 ± 0.04	$< 10^{-5}$
ML ID (mm)	0.59 ± 0.07	0.59 ± 0.05	NS
AP OD (mm)	0.81 ± 0.05	0.93 ± 0.07	< 0.001
AP ID (mm)	0.35 ± 0.04	0.48 ± 0.08	< 0.001
CSA (mm^2)	0.49 ± 0.06	0.67 ± 0.05	$< 10^{-5}$
I (mm^4)	0.041 ± 0.009	0.079 ± 0.011	$< 10^{-6}$
Ash Percentage	68.6 ± 1.0	70.2 ± 1.5	NS
Failure Load (N)	7.9 ± 1.4	8.1 ± 0.9	NS
Structural Stiffness (N/mm)	22 ± 7	23 ± 5	NS
Failure Stress (MPa)	192 ± 36	118 ± 13	$< 10^{-4}$
Young's Modulus (MPa)	4800 ± 1570	2610 ± 490	0.002

BMI = body mass, ML = mediolateral, O = outer, D = diameter, I = inner, AP = anteroposterior, I = cross-sectional moment of inertia, N = newtons, MPa = megapascals. The Bonferroni-corrected significance level is 0.004.

FIGURE LEGENDS

Figure 1. FTIR imaging of HcB/23 (top) and HcB/8 (bottom). Left panels show light micrographs of the specimens. Periosteal surface is to the left. The section contains the entire HcB/23 cortical thickness, but not the entire HcB/8 cortical thickness. Center panels show pseudocolor maps of collagen cross link maturity indices. Right panels show histograms of the cross link maturity indices for all the valid pixels.

Figure 2. FTIR imaging of HcB/23 (top) and HcB/8 (bottom). Left panels show light micrographs of the specimens, taken from the same samples as **figure 1**. Periosteal surface is to the left. The section contains the entire HcB/23 cortical thickness, but not the entire HcB/8 cortical thickness. Center panels show pseudocolor maps of crystallinity cross link maturity indices. Right panels show histograms of the cross link maturity indices for all the valid pixels.

Figure 3. Correlation length (in pixels) vs. correlation coefficient. Note that all of the samples have a more or less linear region for small r. HcB/8 = + and HcB/23 = X. The dotted lines show the minimum and maximum linear coefficients relating correlation length and correlation coefficent from the initial, linear portions of the correlation functions.

LITERATURE CITED

1. **Paganini-Hill, A., A. Chao, R.K. Ross, and B.E. Henderson, *Exercise and other factors in the prevention of hip fracture: the Leisure World study.* Epidemiology, 1991. 2(1): p. 16-25.**

2. **Graafmans, W.C., M.E. Ooms, P.D. Bezemer, L.M. Bouter, and P. Lips, *Different risk profiles for hip fractures and distal forearm fractures: a prospective study.* Osteoporos Int, 1996. 6(6): p. 427-31.**

3. **Ross, P.D., J.W. Davis, R.S. Epstein, and R.D. Wasnich, *Pre-existing fractures and bone mass predict vertebral fracture incidence in women.* Ann Intern Med, 1991. 114(11): p. 919-23.**

4. **Kotowicz, M.A., L.J. Melton, 3rd, C. Cooper, E.J. Atkinson, O.F. WM, and B.L. Riggs, *Risk of hip fracture in women with vertebral fracture.* J Bone Miner Res, 1994. 9(5): p. 599-605.**

5. **Wasnich, R.D., J.W. Davis, and P.D. Ross, *Spine fracture risk is predicted by non-spine fractures.* Osteoporos Int, 1994. 4(1): p. 1-5.**

6. **Cummings, S.R., M.C. Nevitt, W.S. Browner, K. Stone, K.M. Fox, K.E. Ensrud, J. Cauley, D. Black, and T.M. Vogt, *Risk factors for hip fracture in white women. Study of Osteoporotic Fractures Research Group.* N Engl J Med, 1995. 332(12): p. 767-73.**

7. **Hayes, W., *Basic Biomechanics of the Skeleton*, in *Current Concepts of Bone Fragility*. 1986, Springer-Verlag: Heidelberg. p. 3-18.**

8. **Turner, C.H., and D.B. Burr, *Basic biomechanical measurements of bone: a tutorial.* Bone, 1993. 14(4): p. 595-608.**

9. **Faulkner, K.G., S.R. Cummings, D. Black, L. Palermo, C.C. Gluer, and H.K. Genant, *Simple measurement of femoral geometry predicts hip fracture: the study of osteoporotic fractures.* J Bone Miner Res, 1993. 8(10): p. 1211-7.**

10. **Cummings, S.R., J.A. Cauley, L. Palermo, P.D. Ross, R.D. Wasnich, D. Black, and K.G. Faulkner, *Racial differences in hip axis lengths might explain racial differences in rates of hip fracture. Study of Osteoporotic Fractures Research Group.* Osteoporos Int, 1994. 4(4): p. 226-9.**

11. **Gluer, C.C., S.R. Cummings, A. Pressman, J. Li, K. Gluer, K.G. Faulkner, S. Grampp, and H.K. Genant, *Prediction of hip fractures from pelvic radiographs: the study of osteoporotic fractures. The Study of Osteoporotic Fractures Research Group.* J Bone Miner Res, 1994. 9(5): p. 671-7.**

12. **Nakamura, T., C.H. Turner, T. Yoshikawa, C.W. Slemenda, M. Peacock, D.B. Burr, Y. Mizuno, H. Orimo, Y. Ouchi, and C.J. Johnston, *Do variations in hip geometry explain differences in hip fracture risk between Japanese and white Americans?* J Bone Miner Res, 1994. 9(7): p. 1071-6.**

13. **Boonen, S., R. Koutri, J. Dequeker, J. Aerssens, G. Lowet, J. Nijs, G. Verbeke, E. Lesaffre, and P. Geusens, *Measurement of femoral geometry in type I and type II osteoporosis: differences in hip axis length consistent with heterogeneity in the pathogenesis of osteoporotic fractures.* J Bone Miner Res, 1995. 10(12): p. 1908-12.**

14. **Mikhail, M.B., A.N. Vaswani, and J.F. Aloia, *Racial differences in femoral dimensions and their relation to hip fracture.* Osteoporos Int, 1996. 6(1): p. 22-4.**

15. **Karlsson, K.M., I. Sernbo, K.J. Obrant, I. Redlund-Johnell, and O. Johnell, *Femoral neck geometry and radiographic signs of osteoporosis as predictors of hip fracture.* Bone, 1996. 18(4): p. 327-30.**

16. **Bell, K.L., N. Loveridge, J. Power, N. Garrahan, M. Stanton, M. Lunt, B.F. Meggitt, and J. Reeve, *Structure of the femoral neck in hip fracture: cortical bone loss in the inferoanterior to superoposterior axis.* J Bone Miner Res, 1999. 14(1): p. 111-9.**

17. **Bell, K.L., N. Loveridge, J. Power, N. Garrahan, B.F. Meggitt, and J. Reeve, *Regional differences in cortical porosity in the fractured femoral neck.* Bone, 1999. 24(1): p. 57-64.**

18. **Beck, T.J., T.L. Oreskovic, K.L. Stone, C.B. Ruff, K. Ensrud, M.C. Nevitt, H.K. Genant, and S.R. Cummings, *Structural adaptation to changing skeletal load in the progression toward hip fragility: the study of osteoporotic fractures.* J Bone Miner Res, 2001. 16(6): p. 1108-19.**

19. **Beck, T.J., C.B. Ruff, W.W. Scott, Jr., C.C. Plato, J.D. Tobin, and C.A. Quan, *Sex differences in geometry of the femoral neck with aging: a structural analysis of bone mineral data.* Calcif Tissue Int, 1992. 50(1): p. 24-9.**

20. **Beck, T.J., C.B. Ruff, and K. Bissessur, *Age-related changes in female femoral neck geometry: implications for bone strength.* Calcif Tissue Int, 1993. 53(Suppl 1): p. S41-6.**

21. **Bass, S., P.D. Delmas, G. Pearce, E. Hendrich, A. Tabensky, and E. Seeman, *The differing tempo of growth in bone size, mass, and density in girls is region-specific.* J Clin Invest, 1999. 104(6): p. 795-804.**

22. **Duan, Y., C.H. Turner, B.T. Kim, and E. Seeman, *Sexual dimorphism in vertebral fragility is more the result of gender differences in age-related bone gain than bone loss.* J Bone Miner Res, 2001. 16(12): p. 2267-75.**

23. **Majumdar, S., M. Kothari, P. Augat, D.C. Newitt, T.M. Link, J.C. Lin, T. Lang, Y. Lu, and H.K. Genant, *High-resolution magnetic resonance imaging: three-dimensional trabecular bone architecture and biomechanical properties.* Bone, 1998. 22(5): p. 445-54.**

24. **Kabel, J., A. Odgaard, B. van Rietbergen, and R. Huiskes, *Connectivity and the elastic properties of cancellous bone.* Bone, 1999. 24(2): p. 115-20.**

25. **Uchiyama, T., T. Tanizawa, H. Muramatsu, N. Endo, H.E. Takahashi, and T. Hara, *Three-dimensional microstructural analysis of human trabecular bone in relation to its mechanical properties.* Bone, 1999. 25(4): p. 487-91.**

26. **Chappard, D., E. Legrand, B. Haettich, G. Chales, B. Auvinet, J.P. Eschard, J.P. Hamelin, M.F. Basle, and M. Audran, *Fractal dimension of trabecular bone: comparison of three histomorphometric computed techniques for measuring the architectural two-dimensional complexity.* J Pathol, 2001. 195(4): p. 515-21.**

27. **Akhter, M.P., U.T. Iwaniec, M.A. Covey, D.M. Cullen, D.B. Kimmel, and R.R. Recker, *Genetic variations in bone density, histomorphometry, and strength in mice.* Calcif Tissue Int, 2000. 67(4): p. 337-44.**

28. **Jepsen, K.J., D.E. Pennington, Y.L. Lee, M. Warman, and J. Nadeau, *Bone brittleness varies with genetic background in A/J and C57BL/6J inbred mice.* J Bone Miner Res, 2001. 16(10): p. 1854-62.**

29. **Turner, C.H., Y.F. Hsieh, R. Muller, M.L. Bouxsein, C.J. Rosen, M.E. McCrann, L.R. Donahue, and W.G. Beamer, *Variation in bone biomechanical properties, microstructure, and density in BXH recombinant inbred mice.* J Bone Miner Res, 2001. 16(2): p. 206-13.**

30. **Yershov, Y., T.H. Baldini, S. Villagomez, T. Young, M.L. Martin, R.S. Bockman, M.G.E. Peterson, and R.D. Blank, *Bone Strength and Related Traits in HcB/Dem Recombinant Congenic Mice.* J Bone Miner Res, 2001. 16: p. ???**

31. **Marcott, C., R.C. Reeder, E.P. Paschalis, D.N. Tatakis, A.L. Boskey, and R. Mendelsohn, *Infrared microspectroscopic imaging of biomineralized tissues using a mercury-cadmium-telluride focal-plane array detector.* Cell Mol Biol (Noisy-le-grand), 1998. 44(1): p. 109-15.**

32. **Mendelsohn, R., E.P. Paschalis, and A.L. Boskey, *Infrared Spectroscopy, Microscopy, and Microscopic Imaging of Mineralizing Tissues. Spectra-Structure Correlations from Human Iliac Crest Biopsies.* Biomed Optics, 1999. 4(1): p. 14-21.**

33. **Demant, P., and A.A. Hart, *Recombinant congenic strains--a new tool for analyzing genetic traits determined by more than one gene.* Immunogenetics, 1986. 24(6): p. 416-22.**

34. **Moen, C.J., M.A. van der Valk, M. Snoek, B.F. van Zutphen, O. von Deimling, A.A. Hart, and P. Demant, *The recombinant congenic strains--a novel genetic tool applied to the study of colon tumor development in the mouse.* Mamm Genome, 1991. 1(4): p. 217-27.**

35. **van Zutphen, L.F., M. Den Bieman, A. Lankhorst, and P. Demant, *Segregation of genes from donor strain during the production of recombinant congenic strains.* Lab Anim, 1991. 25(3): p. 193-7.**

36. **Groot, P.C., C.J. Moen, W. Dietrich, J.P. Stoye, E.S. Lander, and P. Demant, *The recombinant congenic strains for analysis of multigenic traits: genetic composition.* Faseb J, 1992. 6(10): p. 2826-35.**

37. **Stassen, A.P., P.C. Groot, J.T. Eppig, and P. Demant, *Genetic composition of the recombinant congenic strains.* Mamm Genome, 1996. 7(1): p. 55-8.**

38. **Taylor, B.A., *Recombinant inbred strains: use in gene mapping*, in *Origins of Inbred Mice*, H.C. Morse, Editor. 1978, Academic Press: New York. p. 423-438.**

39. **Bailey, D.W., *Recombinant inbred strains and bilineal congenic strains*, in *The Mouse in Biomedical Research*, H.L. Foster, J.D. Small, and J.G. Fox, Editors. 1981, Academic Press: New York. p. 223-239.**

40. **Donnelly, R., R. Bockman, E. Di Carlo, F. Betts, and A. Boskey, *The effect of gallium nitrate on healing of vitamin D- and phosphate-deficient rickets in the immature rat.* Calcif Tissue Int, 1993. 53(6): p. 400-10.**

41. **Camacho, N.P., C.M. Rimnac, R.A.J. Meyer, S. Doty, and A.L. Boskey, *Effect of abnormal mineralization on the mechanical behavior of X-linked hypophosphatemic mice femora.* Bone, 1995. 17(3): p. 271-278.**

42. **Simske, S.J., M.W. Luttges, and H. Wachtel. *Age dependent development of osteopenia in the long bones of tail-suspended mice.* in *ISA*. 1990.**

43. **Ferretti, J.L., E.P. Spiaggi, R. Capozza, G. Cointry, and J.R. Zanchetta, *Interrelationships between geometric and mechanical properties of long bones from***

three rodent species with very different biomass: phylogenetic implications. **J Bone Miner Res, 1992. 7(S2): p. S433-S435.**

44. Paschalis, E.P., F. Betts, E. DiCarlo, R. Mendelsohn, and A.L. Boskey, *FTIR microspectroscopic analysis of human iliac crest biopsies from untreated osteoporotic bone.* Calcif Tissue Int, 1997. 61(6): p. 487-92.

45. Paschalis, E.P., K. Verdelis, S.B. Doty, A.L. Boskey, R. Mendelsohn, and M. Yamauchi, *Spectroscopic characterization of collagen cross-links in bone.* J Bone Miner Res, 2001. 16(10): p. 1821-8.

46. Yershov, Y., T.H. Baldini, S. Villagomez, T. Young, M.L. Martin, R.S. Bockman, M.G. Peterson, and R.D. Blank, *Bone strength and related traits in HcB/Dem recombinant congenic mice.* J Bone Miner Res, 2001. 16(6): p. 992-1003.

47. Gadaleta, S.J., E.P. Paschalis, F. Betts, R. Mendelsohn, and A.L. Boskey, *Fourier transform infrared spectroscopy of the solution-mediated conversion of amorphous calcium phosphate to hydroxyapatite: new correlations between X-ray diffraction and infrared data.* Calcif Tissue Int, 1996. 58(1): p. 9-16.

48. Meunier, P.J., and G. Boivin, *Bone mineral density reflects bone mass but also the degree of mineralization of bone: therapeutic implications.* Bone, 1997. 21(5): p. 373-7.

49. Boivin, G.Y., P.M. Chavassieux, A.C. Santora, J. Yates, and P.J. Meunier, *Alendronate increases bone strength by increasing the mean degree of mineralization of bone tissue in osteoporotic women.* Bone, 2000. 27(5): p. 687-94.

50. Aparicio, S., S.B. Doty, N.P. Camacho, E.P. Paschalis, L. Spevak, R. Mendelsohn, and A.L. Boskey, *Optimal Methods for Processing Mineralized Tissues for Fourier Transform Infrared Microspectroscopy.* Calc Tiss Int, 2001. 69: p. 94-101.

51. **Cassella, J.P., R. Pereira, J.S. Khillan, D.J. Prockop, N. Garrington, and S.Y. Ali, *An ultrastructural, microanalytical, and spectroscopic study of bone from a transgenic mouse with a COL1.A1 pro-alpha-1 mutation.* Bone, 1994. 15(6): p. 611-9.**

52. **Landis, W.J., *The strength of a calcified tissue depends in part on the molecular structure and organization of its constituent mineral crystals in their organic matrix.* Bone, 1995. 16(5): p. 533-44.**

53. **Masse, P.G., C.M. Rimnac, M. Yamauchi, S.P. Coburn, R.B. Rucker, D.S. Howell, and A.L. Boskey, *Pyridoxine deficiency affects biomechanical properties of chick tibial bone.* Bone, 1996. 18(6): p. 567-74.**

54. **Camacho, N.P., L. Hou, T.R. Toledano, W.A. Ilg, C.F. Brayton, C.L. Raggio, L. Root, and A.L. Boskey, *The material basis for reduced mechanical properties in oim mice bones.* J Bone Miner Res, 1999. 14(2): p. 264-72.**

Figure 1

COLLAGEN Pyr/DHLNL

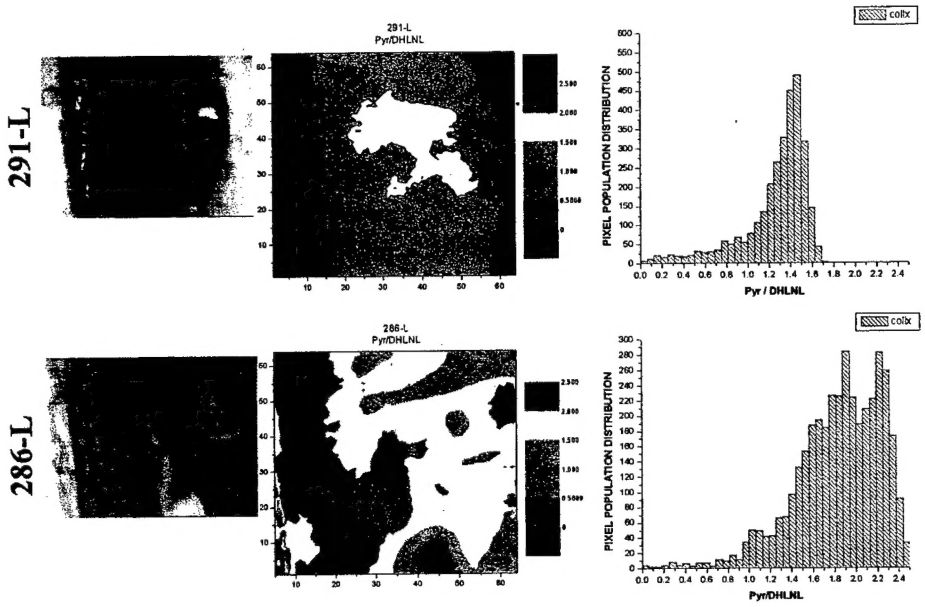

Figure 2

MINERAL CRYSTALLINITY

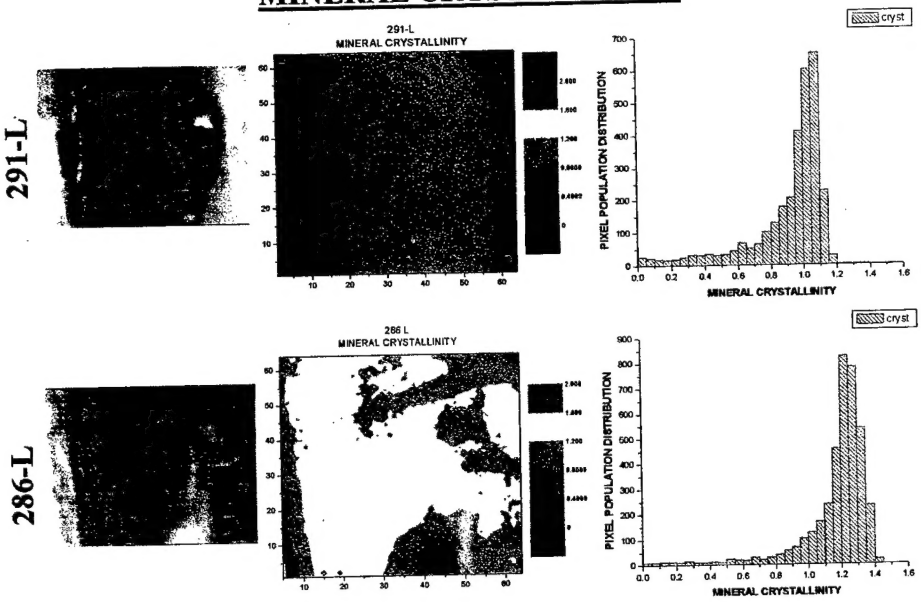

Fig 3

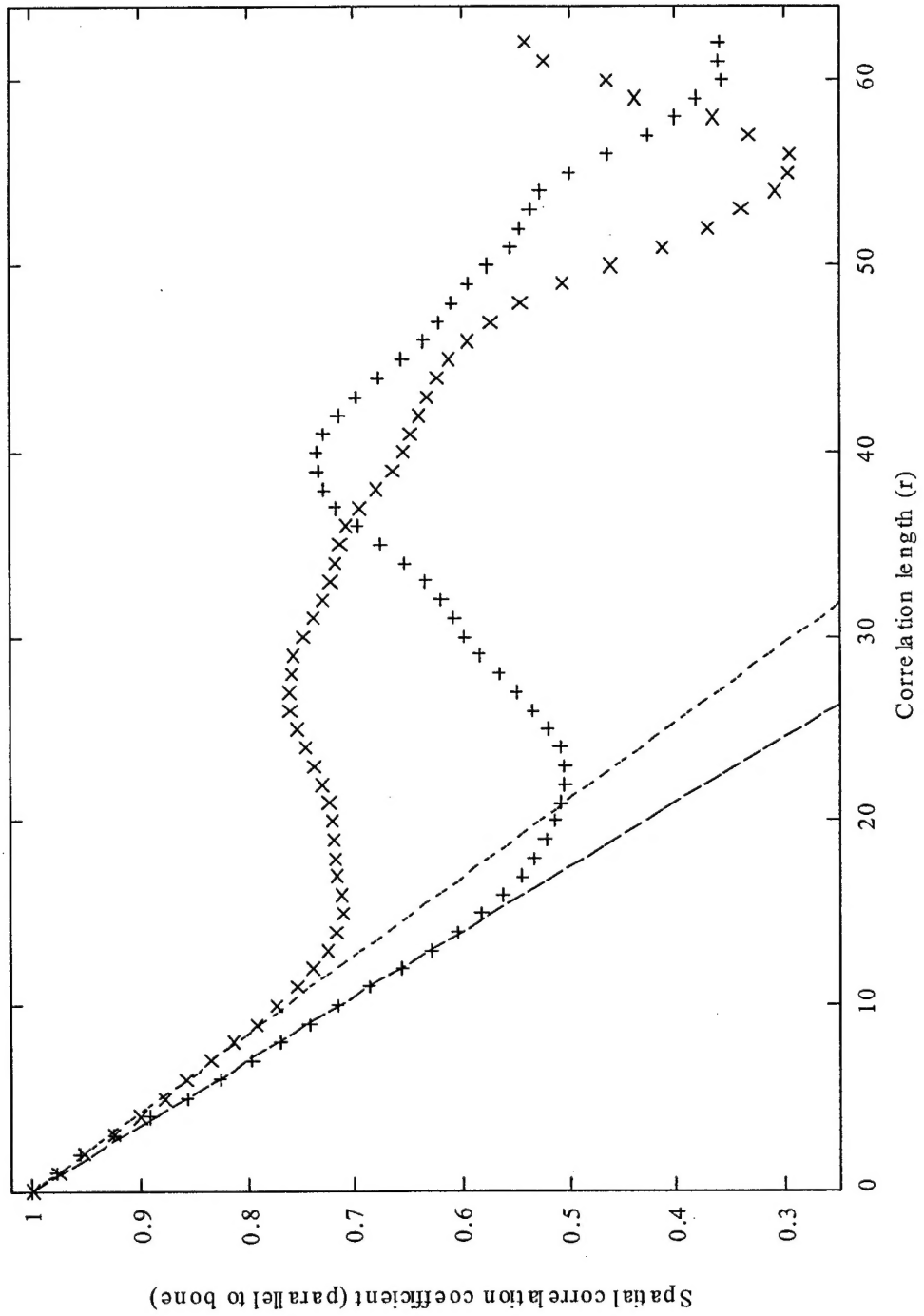
Spatial correlation coefficient (parallel to bone)
1
0.9
0.8
0.7
0.6
0.5
0.4
0.3
Correlation length (r)
0
10
20
30
40
50
60

Collagen Cross-Link Maturity and Crystallinity Indices Differ Markedly in Recombinant Congenic Mice Having Divergent Calculated Tissue Strength

R. D. Blank1, M. Kaufman*2, S. L. Bailey*3, S. N. Coppersmith*2, T. H. Baldini*4, A. L. Boskey5, P. Demant*6, E. P. Paschalis5.
[1]Medicine/Endocrinology, University of Wisconsin, Madison, WI, USA, [2]Physics, University of Wisconsin, Madison, WI, USA, [3]Physics, College of William & Mary, Williamsburg, VA, USA, [4]Biomechanics and Biomaterials, University of Colorado, Boulder, CO, USA, [5]Research Division, Hospital for Special Surgery, New York, NY, USA, [6]Genetics, Netherlands Cancer Institute, Amsterdam, Netherlands.

The structural strength of a bone can be partitioned into architectural and material components. In 3-point bending tests of 6 month old female humeri from the HcB/Dem recombinant congenic series, 2 strains differed markedly in calculated failure stress as summarized in the table. We used Fourier Transform Infrared Spectroscopic Imaging (FTIRI) to determine whether differences in collagen cross-link maturity, crystallinity, or spatial ordering could account for the large difference in calculated tissue strength between these 2 strains with similar mineral content. Cross-link maturity and crystallinity were assayed as the absorbance ratios at 1660:1690 cm^{-1} and 1030:1020 cm^{-1}, respectively. One-dimensional spatial correlation functions were estimated to compare the uniformity of the indices within fields. For HcB/8, the mean cross-link maturity index is 1.654 and the median is 1.641. The mean and median HcB/23 cross-link maturity indices are 1.273 and 1.365, respectively. The difference in cross link maturity is highly significant ($\chi^2 = 1968$, 9 df, $P < 10^{-15}$). For HcB/8, the mean and median crystallinity index are 0.950 and 0.974, respectively. In HcB/23, the corresponding values are 0.840 and 0.909. As for cross link maturity, the difference between the strains is highly significant ($\chi^2 = 400$, 6 df, $P < 10^{-15}$). Cross-link maturity and crystallinity are highly and similarly correlated in both strains, with correlation coeffecients of 0.751 for HcB/8 and 0.758 for HcB/23 ($P < 10^{-16}$ in both strains). We did not find evidence of significant differences between the strains' 1-dimensional spatial correlation functions. The high correlation between cross-link maturity and crystallinity reflects the interdependence of the protein and mineral elements of bone matrix. The data illustrate the usefulness of FTIRI to examine bone quality and relate it to biomechanical performance.

Anatomic and Biomechanical Performance of HcB/8 and HcB/23 Mice

	HcB/8 (N=10)	**HcB/23** (N=9)	**P value**
Body Mass (g)	19.9 ± 1.5	23.5 ± 1.1	$< 10^{-4}$
Humeral Length (mm)	11.1 ± 0.3	11.3 ± 0.2	NS
I (mm^4)	0.041 ± 0.009	0.079 ± 0.011	$< 10^{-6}$
Failure Load (N)	7.9 ± 1.4	8.1 ± 0.9	NS
Structural Stiffness (N/mm)	22 ± 7	23 ± 5	NS
Ash Percentage	68.6 ± 1.0	70.2 ± 1.5	NS
Failure Stress (MPa)	192 ± 36	118 ± 13	$< 10^{-4}$